WAVELET DOMAIN COMMUNICATION SYSTEM (WDCS): PACKET-BASED WAVELET SPECTRAL ESTIMATION AND M-ARY SIGNALING

THESIS

Marion Jay F. Lee, First Lieutenant, USAF

AFIT/GE/ENG/02M-14

DEPARTMENT OF THE AIR FORCE
AIR UNIVERSITY

AIR FORCE INSTITUTE OF TECHNOLOGY

Wright-Patterson Air Force Base, Ohio

Report Documentation Page

Report Date	**Report Type**	**Dates Covered (from... to)**
7 Mar 02	Final	Jun 01 - Mar 02

Title and Subtitle Wavelet Domain Communication System (WDCS): Packet-Based Wavelet Spectral Estimation and M-ARY Signaling	**Contract Number**
	Grant Number
	Program Element Number
Author(s) 1st Lt Marion Jay F. Lee, USAF	**Project Number**
	Task Number
	Work Unit Number
Performing Organization Name(s) and Address(es) Air Force Institute of Technology Graduate School of Engineering and Management (AFIT/EN) 2950 P Street, Bldg 640 WPAFB OH 45433-7765	**Performing Organization Report Number** AFIT/GE/ENG/02M-14
Sponsoring/Monitoring Agency Name(s) and Address(es) AFRL/SNRW Mr. James P. Stephens 2241 Avionics CL, Bldg 620, Rm N2L3 WPAFDB OH 45433-7765	**Sponsor/Monitor's Acronym(s)**
	Sponsor/Monitor's Report Number(s)
Distribution/Availability Statement Approved for public release, distribution unlimited	
Supplementary Notes	

Abstract
A recently proposed Wavelet Domain Communication System (WDCS) using transform domain processing demonstrated excellent interference avoidance capability under adverse environmental conditions. This work extends previous results by 1) incorporating a wavelet packet decomposition technique, 2) demonstrating M-Ary signaling capability, and 3) providing increased adaptivity over a larger class of interference signals. The newly proposed packet-based WDCS is modeled and its performance characterized using MATLABâ. In addition, the WDCS response to two scenarios simulating Doppler effects and physical separation of transceivers are obtained. The fundamental metric for analysis and performance evaluation is bit error rate (Pb). Relative to the previous non-packet WDCS, the proposed packet-based WDCS provides improved/comparable bit error performance in several interference scenarios single-tone, multiple-tone, swept-tone, and partial band interference is considered. Interference avoidance capability was characterized for a bit energy-to-noise power level (Eb/N0) of 4.0 dB and interference energy-to-signal energy (I/E) ratios ranging from 0.0 dB to 16.0 dB. For binary, 4-Ary, and 8-Ary CSK data modulations, the packet-based WDCS exhibited average Pb improvements of 6.7, 9.2, and 12.0 dB, respectively, for partial band and swept-tone interference. For single and multiple-tone interference, improvements of 8.0, 12.4, and 15.7 dB were realized. Furthermore, bit error sensitivity analyses indicate the WDCS communicates effectively under non-ideal real-world conditions (transceivers located in dissimilar environments) while exhibiting average Pb improvements of 5.4, 5.1, and 5.8 dB, relative to systems having no interference suppression.

Subject Terms
Interference Avoidance, Transform Domain, Wavelet Domain, Wavelets, Wavelet Packets, Communication, Cyclic Shift Keying

Report Classification	**Classification of this page**
unclassified	unclassified
Classification of Abstract	**Limitation of Abstract**
unclassified	UU

Number of Pages
95

The views expressed in this thesis are those of the author and do not reflect the official policy or position of the United States Air Force, Department of Defense or the U.S. Government.

AFIT/GE/ENG/02M-14

WAVELET DOMAIN COMMUNICATION SYSTEM (WDCS): PACKET-BASED WAVELET SPECTRAL ESTIMATION AND M-ARY SIGNALING

THESIS

Presented to the Faculty

Department of Electrical and Computer Engineering

Graduate School of Engineering and Management

Air Force Institute of Technology

Air University

Air Education and Training Command

In Partial Fulfillment of the Requirements for the

Degree of Master of Science in Electrical Engineering

Marion Jay F. Lee, B.S.E.E

First Lieutenant, USAF

March 2002

AFIT/GE/ENG/02M-14

WAVELET DOMAIN COMMUNICATION SYSTEM (WDCS):
PACKET-BASED WAVELET SPECTRAL ESTIMATION AND M-ARY SIGNALING

Marion Jay F. Lee, B.S.E.E
First Lieutenant, USAF

Approved:

Michael A. Temple, Ph.D. Committee Chairman	6 Mar 02 date
Roger L. Claypoole Jr., Ph.D., Major, USAF Committee Member	6 MAR 02 date
Richard A. Raines, Ph.D. Committee Member	6 Mar 02 date

Acknowledgments

I want to express my sincere appreciation to several people for their continuous support and guidance that made this research a rewarding and enjoyable experience. First to Dr. Michael A. Temple, my thesis advisor, for your motivation, guidance, and 'heading checks', thank you. Second to Major Roger L. Claypoole and Dr. Richard A. Raines, my thesis committee members, thank you for your professional counsel and support. To my fellow students and their families, thank you for taking me in and making me feel welcome. Special thanks to Matt and Kevin for lending an ear whenever prompted, but most of all thank you for your friendship. Finally, I would like to thank my family for their support throughout my studies at AFIT.

Marion Jay F. Lee

Table of Contents

Page

List of Figures

List of Tables

Abstract

A recently proposed Wavelet Domain Communication System (WDCS) using transform domain processing demonstrated excellent interference avoidance capability under adverse environmental conditions. This work extends previous results by 1) incorporating a wavelet packet decomposition technique, 2) demonstrating *M-Ary* signaling capability, and 3) providing increased adaptivity over a larger class of interference signals. The newly proposed packet-based WDCS is modeled and its performance characterized using MATLAB®. In addition, the WDCS response to two scenarios simulating Doppler effects and physical separation of transceivers are obtained. The fundamental metric for analysis and performance evaluation is bit error rate (P_b). Relative to the previous non-packet WDCS, the proposed packet-based WDCS provides improved/comparable bit error performance in several interference scenarios – single-tone, multiple-tone, swept-tone, and partial band interference is considered. Interference 'avoidance' capability was characterized for a bit energy-to-noise power level (E_b/N_0) of 4.0 dB and interference energy-to-signal energy (I/E) ratios ranging from 0.0 dB to 16.0 dB. For binary, 4-*Ary*, and 8-*Ary* CSK data modulations, the packet-based WDCS exhibited average P_b improvements of 6.7, 9.2, and 12.0 dB, respectively, for partial band and swept-tone interference. For single and multiple-tone interference, improvements of 8.0, 12.4, and 15.7 dB were realized. Furthermore, bit error sensitivity analyses indicate the WDCS communicates effectively under non-ideal 'real-world' conditions (transceivers located in dissimilar environments) while exhibiting average P_b improvements of 5.4, 5.1, and 5.8 dB, relative to systems having no interference suppression.

WAVELET DOMAIN COMMUNICATION SYSTEM (WDCS):

PACKET-BASED WAVELET SPECTRAL ESTIMATION AND M-ARY SIGNALING

1 Introduction

1.1 Background

Reliable communications is essential for conducting day-to-day business in both the military and commercial sectors. For the most part, the equipment used for conducting such communications shares much commonality. However, most military communication systems must be designed to operate in the presence of intentional interference or jamming. The primary objective for an interferer is to degrade or disrupt communication system performance to the point where it is no longer considered reliable. With reference to a digital communication system, reliability is considered lost when an excessive number of bits are received in error. A principal contributor to increased bit error rate is channel interference, both intentional and/or unintentional. Therefore, communication research primarily focuses on ensuring the ability to circumvent channel interference.

Various modulation techniques have been developed to mitigate interference effects, some of which are examined in this section. Two developmental communication systems demonstrating interference avoidance capabilities are introduced, namely, the

Transform Domain Communication System (TDCS) and the Wavelet Domain Communication System (WDCS) [1, 2]. The TDCS and WDCS are specifically designed to operate successfully in an environment containing adverse, intentional interference.

Unintentional interference generally implies low-level interference with the most rudimentary source being Additive White Gaussian Noise (AWGN), i.e., noise having a constant power spectral density (PSD) over all frequencies. All communication systems must contend with and overcome AWGN effects to operate effectively. Any system operating within, or producing harmonic energy within, the spectral regions of interest are additional sources of unintentional interference, e.g., radio stations, television stations, cellular telephones, navigational aids, and radars may represent a significant source of unintentional interference.

Intentional interference can be broadly defined as a radiation source having sufficient energy (on the order of the desired signal energy) that is deliberately targeted at a communications system with the sole function of disrupting system operation. Such interference may be classified as either narrowband or wideband; the distinction is made depending on the relative amount of bandwidth the interference occupies in relation to the system bandwidth. Narrowband interference typically occupies a range of frequencies representing some fractional percentage of the overall system bandwidth. Four types of narrowband interference considered in this research include: single-tone, multiple-tone, swept-tone, and partial-band noise interference. One assumption commonly made to provide objective evaluation of narrowband interference effects is that the interferer has a finite, fixed amount of energy in all interference cases. With this in mind, single-tone interference confines all energy to a single sinusoidal frequency and

can be the most disruptive if properly located. Multiple-tone interference contains multiple, single frequency sinusoidal tones distributed within the system bandwidth. In the case of fixed interference power, each of these tones contains less energy per frequency than the single-tone interference and is generally not as effective. For swept-tone interference, a single-tone frequency changes as a function of time and can be as disruptive as stationary single-tone interference. Partial-band noise interference spans a contiguous range of frequencies (fractional percentage of the system bandwidth) and possesses characteristics that are representative of bandlimited AWGN.

Wideband interference spreads energy over the entire system bandwidth, effectively raising the system noise floor. The effects of broadband interference are perhaps the best understood with performance degradation analysis closely paralleling channel noise analysis. In general, narrowband interference is the most disruptive. Therefore, the focus of this research is on minimizing the effects of narrowband interference through interference avoidance, i.e., excising the interference from the detection and estimation process.

Historically, time-domain signal-processing techniques have been used to minimize interference effects through *a priori* selection of transmitted waveform shapes and receiver demodulation techniques for achieving desired performance over a given communication channel (assumed AWGN for the most part). Given a specific transmitted waveform, signal demodulation at the receiver can be accomplished by time-domain signal processing techniques such as matched filtering, or equivalently correlation, which can be shown optimal for signaling over an AWGN channel. For this non-adaptive constrained mode of operation, system performance becomes sub-optimal

when interference is introduced into the channel, i.e., the transmitter and receiver continue to operate as designed but must also deal with the perturbed frequency domain characteristics of the channel. Two major steps have greatly aided the growth of transform domain signal processing and communication techniques, including, 1) the development of devices and techniques for performing near "real-time" Fourier transforms and 2) a shift in design philosophy and the evolution from *interference suppression* to *interference avoidance*, i.e., a movement away from the *a priori* design methodology based on anticipated channel characteristics to the real-time generation of waveforms that avoid spectral regions containing interference. The remainder of this section provides a brief overview of the evolutionary process.

The first major step towards implementing transform-domain signal processing came in 1978 when Milstein, et.al., demonstrated a Surface Acoustic Wave (SAW) device that could perform near real-time Fourier transformations and inversions. Additionally, it was shown that ideal filtering, unrealizable with time-domain processing, could be developed in the frequency domain, a process known as *Transform Domain* (TD) processing. With this discovery, bandpass and notch TD filters were constructed and shown to effectively remove interference. Although the primary focus of this early research was on Fourier transforms, other transforms were identified as potential candidates for SAW implementation [3]. In 1982, Milstein, et.al., applied transform domain filtering techniques to a spread spectrum communications system and demonstrated approximately 10 dB of processing gain improvement relative to a conventional spread spectrum system [4].

The second major step involved a shift in design philosophy and a revolutionary change in interference rejection methodology. The practice of interference suppression, i.e., minimizing the effects of interference in the receiver, gave way to the concept of *interference avoidance*, i.e., identifying and excising interference at both the transmitter and receiver location such that generated communication waveforms are "tailored" to avoid channel interference. Classical interference suppression at the receiver not only removes the interference but also a portion of the desired information signal energy. If the transmitted information signal can be specifically designed to avoid spectral regions containing interference, and the receiver employs a detection / estimation process that avoids the interference as well, the advantages of TD filtering can be captured without detrimentally suppressing the desired signal energy. In 1989, German analyzed a spread spectrum system employing TD processing at both the transmitter and receiver location [5]. Two years later, the Andren/Harris corporation patented a Low Probability of Intercept (LPI) communication system employing techniques similar to those proposed by German [6]. Both systems use TD processing to completely avoid spectral regions containing interference. The first developmental TDCS model was implemented at the Air Force Institute of Technology (AFIT) in 1996. Radcliffe generated a model in MATLAB® to simulate and characterize performance of the TDCS defined by the Andren/Harris Corp and German [1].

Radcliffe's work shows the level of improvement achievable with a TDCS relative to a conventional Direct Sequence Spread Spectrum (DSSS) system for the interference scenarios previously described [1]. In 1999, Swackhammer demonstrated that Radcliffe's TDCS model was capable of operating in a multiple access

environment [7]. In 2000, Roberts adopted Radcliffe's work and examined TDCS synchronization capabilities, perhaps the most challenging task of all when compared with conventional communication systems using *a priori* waveform structure – previous research assumed perfect synchronization [1, 7, 8]. Synchronization is required before information can be effectively communicated and is consequently a critical step in the communication process. Roberts' work was limited to addressing coarse synchronization, often referred to as acquisition. Once a TDCS achieves coarse synchronization, the system can proceed directly to demodulation and subsequent framing of estimated data. Roberts' results show that the TDCS is capable of achieving coarse synchronization with input Signal-to-Noise Ratios (SNRs) as low as minus 23.0 dB [9].

Further progress in TDCS development was made in 2001 when Klein modified Radcliffe's work by replacing the Fourier-based spectral estimation function with a Wavelet-based technique, giving birth to the Wavelet Domain Communication System (WDCS). WDCS interference avoidance capability was successfully demonstrated while achieving suppression performance comparable to the original TDCS. In addition, introduction of the Wavelet transform offered increased performance for non-stationary signals, e.g., swept-tone interference. Klein concluded that WDCS spectral estimation could be further improved by replacing the original Wavelet processing technique with a Wavelet packet decomposition, indicating potential for more accurate electromagnetic spectral estimates. A recommendation was also made that WDCS research be expanded beyond binary modulation to consider *M-Ary* modulation for increased throughput [2].

1.2 Problem Statement

The ability to consistently produce accurate spectral estimates is essential for successful WDCS operation. The TDCS performance was severely degraded when presented with non-stationary interference, e.g., swept-tone interference. Klein's original WDCS overcame this shortfall and successfully operated in the presence of non-stationary interference with slightly degraded communication performance. As a further improvement, this research considers a wavelet packet decomposition technique to 1) provide more accurate spectral estimation, 2) effectively excise non-stationary interference sources, and 3) expand previous results from binary modulation to include *M-Ary* modulation. The packet-based WDCS performance is characterized under 'real world' electromagnetic environmental conditions, to include a sensitivity analysis of performance degradations due to geographically separated transceivers within non-localized regions, i.e., each transceiver 'sees' a different electromagnetic environment.

1.3 Assumptions

All results and analyses presented as part of this research are based on the following assumptions:

1. The communication channel can be represented as an AWGN source.
2. No multi-path interference exists. Methods exist to handle multi-path and are assumed capable of fully mitigating multi-path effects [10].

3. Two remotely located, geographically separated transceivers can achieve and maintain full synchronization. Although not demonstrated for a WDCS thus far, previous TCDS synchronization work indicates transform domain systems are capable of achieving synchronization [9].
4. Doppler effects are negligible; specifically, the transceivers remain stationary with respect to each other throughout transmission, reception and signal detection.
5. The specific spectral location of the communication signals is not important to this study. Because of the equivalence theorem, analysis of systems employing linear signal processing techniques and frequency translation yield identical results independent of where the information signal is translated and signal processing occurs [11]. Results are generally extendable to any spectral region.
6. Although a two-transceiver scenario is considered, and thus two one-way communication links are effectively present, only the performance of one WDCS link is considered.
7. With the exception of sensitivity analyses, the two transceivers are assumed to be located in a localized geographical region such that they are operating in the same electromagnetic environment.

1.4 Scope

The research presented is limited to analysis, modeling, simulation and developmental testing of a wavelet packet-based spectral estimation process for binary, 4-*Ary*, and 8-*Ary* orthogonal Cyclic Shift Keyed (CSK) data modulations using the WDCS

architecture of [2]. This research closely parallels previous developmental WDCS research, including modeling and simulation of system performance using MATLAB®. The proposed packet-based WDCS bit error (P_b) performance is evaluated under different interference scenarios and compared with previous WDCS results. The sensitivity of WDCS bit error performance is evaluated for scenarios in which the remotely located transceivers 'see' different electromagnetic environments, e.g., environmental changes that may be experienced as a result of varying Doppler shift and attenuation resulting from different separations between each transceiver and the interfering source.

1.5 Approach

The newly proposed packet-based WDCS architecture is built on a previously demonstrated WDCS architecture [12]. The previous WDCS architecture used conventional wavelet techniques and a Daubechies 8 mother wavelet [2, 12] for spectral estimation. The Daubechies 8 mother wavelet was originally chosen since it possessed desirable properties of orthogonality, time-frequency localization, and multi-resolution; it was successfully exploited and clearly demonstrates the potential for using wavelet techniques to improve transform domain performance. For this work, no fundamental changes are made to the original WDCS architecture, i.e., the functionality of each system component remains unchanged - only the internal spectral estimation mechanism is modified such that the original Wavelet processing is replaced with a Wavelet packet decomposition technique.

1.6 Materials and Equipment

All WDCS models and performance simulations were developed in MATLAB® Version 6.0, from The Mathworks Inc., Natick, MA. The simulations were run on Sun Ultra® and Dell Precision workstations in computer labs at the Air Force Institute of Technology (AFIT).

1.7 Thesis Organization

Chapter 2 provides background information on the previous WDCS architecture [2]. The WDCS architecture is presented and accompanied by explanations of key design processes. Previous WDCS research results are specified to establish a benchmark for future performance characterization. Chapter 3 outlines the computer simulation process used for this research, including a brief discussion on the lowpass complex envelope signal representation and the Monte Carlo method. Next, the Wavelet packet decomposition process is outlined and advantages over the basic wavelet decomposition process are provided. Chapter 3 concludes with a presentation of the model verification and validation process. Chapter 4 presents comprehensive simulation results and analyses. Communication and interference scenarios that were simulated for the work are outlined along with corresponding research results. A WDCS performance summary is provided at the end of Chapter 4. Chapter 5 provides an overall research

summary and recommendations for future research. Additional data are provided in the appendices for completeness and includes the MATLAB® code developed for this research.

2 Background

2.1 Introduction

This chapter provides background information on the transform domain (TDCS) and wavelet domain (WDCS) communication systems. These interference avoiding communication systems are based on the concept of spectral estimation and shaping in the transform (Fourier or wavelet) domain, i.e., the communication waveform characteristics are tailored based on the *transformed domain* to provide desired electromagnetic characteristics. Figure 1 and Figure 2 show the general transmitter and receiver architectures, respectively, for the TDCS and WDCS. Except for the shaded blocks, the spectral estimation and inverse transform processes, the system implementations are identical and each block is outlined in detail in Section 2.3.1. Although the *implementation* changes between systems, the *functionality* of each shaded block remains unchanged for the TDCS and WDCS architectures.

2.2 Transform Domain Communication System (TDCS)

The TDCS implementation uses a Fourier transform process in the shaded spectral estimation and inverse transform blocks of Figure 1 and Figure 2, i.e., the localized electromagnetic spectral estimate is produced via a Fourier transform. Analysis of the local spectral characteristics, as determined by examining the resultant spectral estimate, determines an appropriate threshold value. For the TDCS, the threshold is

applied across the spectral estimate and all Fourier coefficients magnitudes exceeding the threshold value are discarded (set to a value of zero), while remaining coefficients are retained (set to a value of one). This nonlinear thresholding process produces the 'notched' magnitude vector, $A'(\omega)$, of ones and zeros (notches). The notched magnitude vector is then phase coded, yielding $B_b(\omega)$, which is subsequently scaled to produce $B(\omega)$. This result is then inverse Fourier transformed to produce the fundamental time domain communications waveform, or *basis function b(t)*. The basis function is stored and data modulated prior to transmission [1, 7, 9].

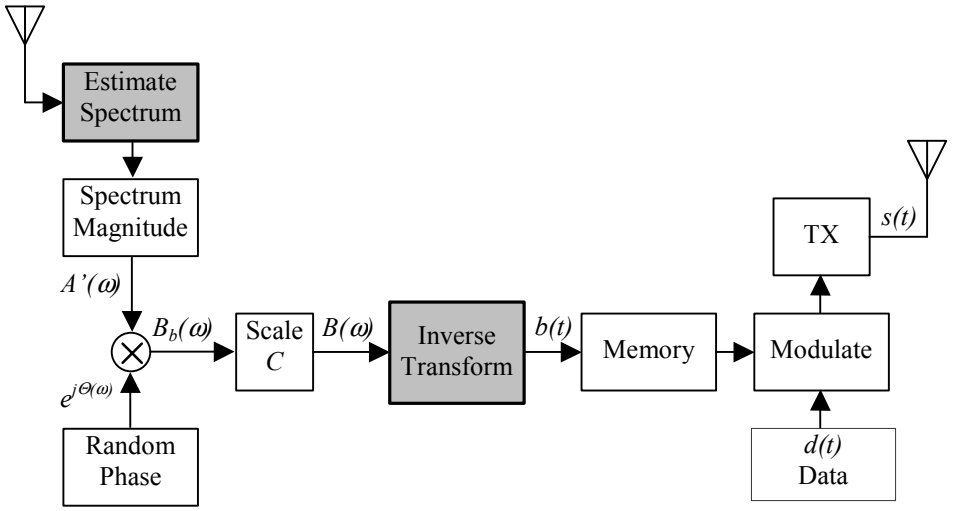

Figure 1. Communication Transmitter Block Diagram [1].

With the exception of the complex conjugation process, the communication receiver structure of Figure 2 generates a local basis function reference, enclosed by the dashed line, in the same manner previously outlined for the transmitter. Under the assumption of ideal signaling conditions, the receiver's reference waveform is assumed identical to the basis function created by the transmitter. Given this assumption, matched

filter performance is realized by correlating the received waveform with specific modulations (*M*- total) of the locally generated reference waveform [1, 7, 9].

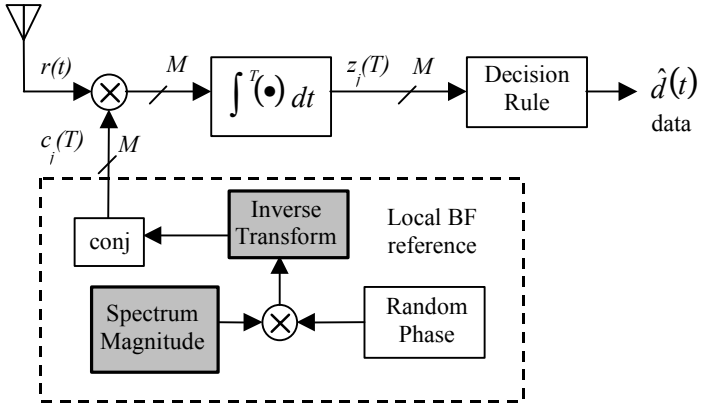

Figure 2. Communication Receiver Block Diagram [1].

2.3 Wavelet Domain Communication System (WDCS)

The WDCS architecture and underlying processes are presented in detail in the following sections. The original WDCS implementation used a traditional wavelet-based transform to perform spectral estimation and was developed to overcome two noted TDCS deficiencies, including 1) the Fourier-based estimator inherently spreads interference energy into adjacent spectral regions not containing interference energy, an inefficiency potentially resulting in degraded performance, and 2) the TDCS fails to effectively estimate the spectral characteristics of non-stationary interference. The original WDCS demonstrated comparable performance to the TDCS for all scenarios

considered. Additionally, the WDCS demonstrated an added capability to effectively estimate non-stationary interference, specifically, swept-tone interference [2].

2.3.1 Traditional Wavelet-Based WDCS Architecture.

The original WDCS architecture simply replaced the Fourier based spectral estimation processes with a traditional wavelet transform. Of necessity, the inverse wavelet transform replaced the inverse Fourier transform. A Daubechies 8 wavelet was chosen in the original work as the 'mother wavelet' because it could serve to form an orthonormal basis and it is compactly supported [2].

The mother wavelet is the fundamental waveform that is scaled and translated to achieve a two-dimensional (time and frequency) parameterization of a signal. Scaling and translation are achieved as shown in (1) where $\psi(t)$ is the mother wavelet and **Z** is the set of all integers. The j and k indices represent the scale and translation, respectively [13].

$$\psi_{j,k}(t) = 2^{j/2}\psi(2^j t - k) \quad j,k \in Z \tag{1}$$

For an orthonormal basis, Parseval's theorem applies and the power in the time-domain signal equals the sum of power in the wavelet coefficients. A compactly supported waveform contains a finite amount of energy concentrated in time, allowing analysis of non-stationary signals [2, 13].

2.3.1.1 Spectral Estimation.

Spectral estimation in the WDCS is accomplished by filtering and decimating the samples of the electromagnetic environment, c_{j+1} in Figure 3 (this is also referred to as a signal decomposition process). In this case, the filter coefficients are computed using the Daubechies 8 wavelet [14].

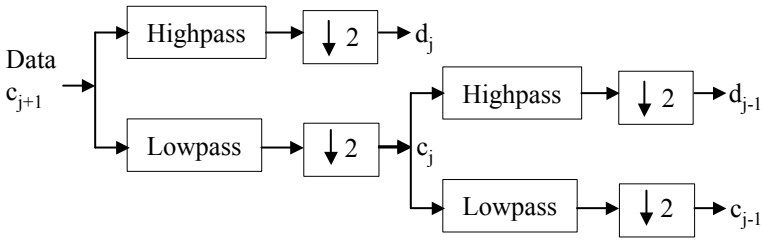

Figure 3. Wavelet Filtering Process [13].

The first iteration of the signal decomposition (filtering and decimating) process divides the data into two sub-bands, the *detailed* and *coarse* sub-bands. Detailed sub-band coefficients, d_j, are the result of passing the data through a highpass filter and decimating, or down-sampling, the filter output by a factor of two. Coarse sub-band coefficients, c_j, are the result of lowpass filtering the data and decimating the filter output by a factor of two. The wavelet decomposition process continues by subsequently splitting and down sampling the lowpass, coarse sub-band coefficients a user-defined number of times. The final output of the iterative decomposition process represents the magnitude of the spectral estimates [2, 13].

2.3.1.2 Thresholding and Spectral Notching.

As illustrated in Figure 1, the thresholding and notching process produces a 'notched' magnitude vector $A'(\omega)$ containing ones and zeros. The pattern of ones and zeros effectively characterizes the desired magnitude of the spectral estimate. For the WDCS implementation, thresholding is performed on a sub-band-by-sub-band basis, i.e., the power contained in each sub-band is independently compared to a predetermined threshold. The threshold value is calculated using the system noise power before introduction of the interference. When sub-band power exceeds the noise power by 20%, interference is declared present and all of the sub-band coefficients are nulled out (set to a value of zero). If sub-band power does not exceed the threshold, all of the sub-band coefficients are retained (set to a value of one). There is no claim of "optimality" with regard to the 20% threshold value, rather, it was empirically chosen and yielded acceptable results in previous research [2, 12].

The number of coefficients contained in each sub-band varies from one to one-half of the original coefficients. This introduces the potential for significantly degraded performance and poor high-frequency interference localization. If after the first iteration of the decomposition process the highpass sub-band power exceeds the threshold, then one-half of the total coefficients are nulled out and high frequency resolution is lost [2, 12]. The inability of the original WDCS to effectively localize high frequency interference is one of the shortcomings addressed in this research.

2.3.1.3 Phase Mapping Process.

Following the thresholding and notching process, the magnitude vector $A'(\omega)$ is phase coded and scaled per (2) by a process called *phase mapping*. In this process, a complex phase vector, $e^{j\phi_i}$, is point multiplied by $A'(\omega)$ to produce $B_b(\omega)$. The phase coded magnitude vector, $B_b(\omega)$, is then scaled by C to achieve the desired symbol energy. The resultant output vector, $B(\omega)$, is then passed to the inverse transform block in Figure 1 to produce the time-domain *basis function*, $b(t)$ [1, 9].

$$B(\omega) = C\,B_b(\omega) = CA'(\omega)\,e^{j\phi_i} \tag{2}$$

The phase code is a maximal-length pseudorandom (PR) sequence produced from a linear feedback shift register (LFSR) as shown in Figure 4. The n-stage LFSR produces an m-sequence of period, or length, equaling $2^n - 1$, i.e., the LFSR output sequence repeats every $2^n - 1$ clock cycles. The r ($r < n$) phase mapper taps correspond to the 2^r possible phase values, e.g., to produce eight phase values, three ($r = 3$) phase mapper taps are used. To simplify analysis, the 2^r phase points are evenly distributed in the complex plane [1, 9].

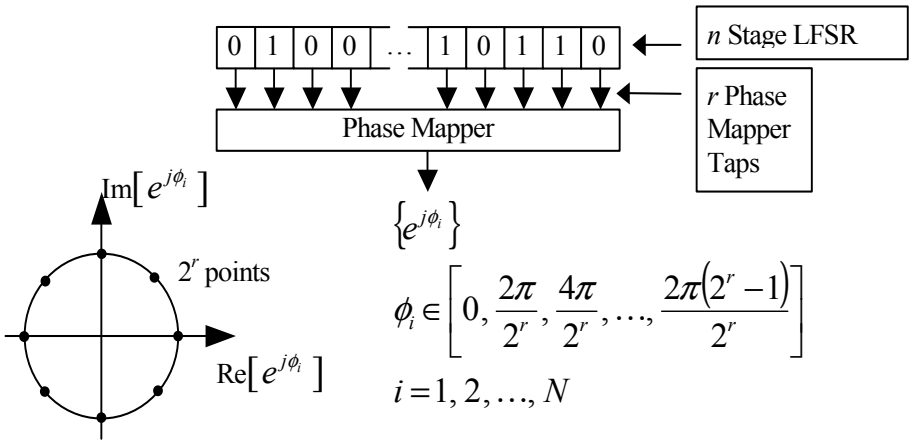

Figure 4. Phase Mapping Diagram [7].

To produce the first phase value, a 'snapshot' of the LFSR contents is mapped to one of the 2^r phase points. The LFSR is then clocked, or shifted, *s* times and a new 'snapshot' is mapped to another phase point. This process repeats a total of N times, where N is the length of the 1xN magnitude vector *A'(ω)*. The resultant phase vector, ϕ_i, has length 2^n, one longer than the *m*-sequence period. For the phase value assignment process described above, the distribution of ϕ_i is nearly uniform on the interval [0,2π) (See Figure 10 in Section 4.2) [1, 2, 7, 9].

2.3.1.4 Basis Function Generation and Modulation.

The output of the phase mapping process, *B(ω)*, is inverse wavelet transformed to produce the time domain basis function *b(t)*. As shown in Figure 1, *b(t)* is stored and subsequently data modulated prior to transmission. A representative WDCS basis function is shown in Figure 5.

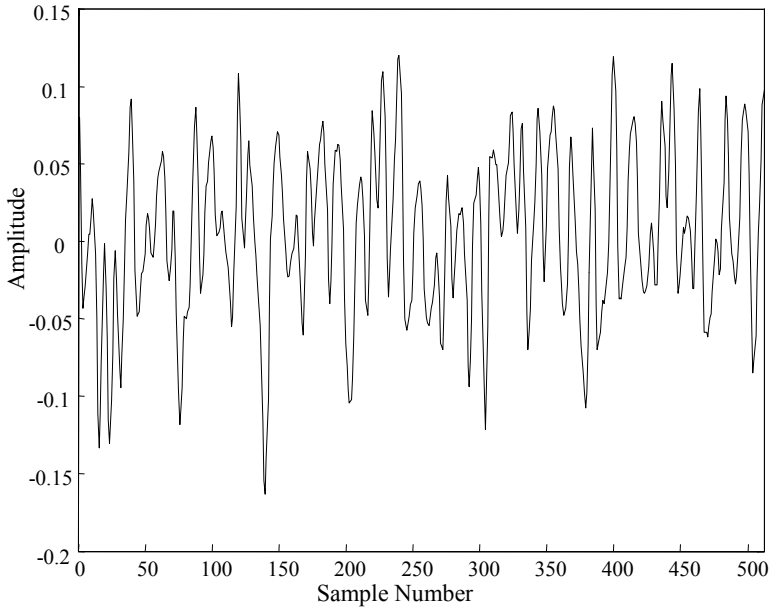

Figure 5. Representative WDCS Basis Function b(t).

As introduced in preliminary WDCS research, Binary Cyclic Antipodal Shift Keying (BCASK) was the form of orthogonal modulation implemented [12]. As reported, BCASK represented a special modified form of BCSK obtained by 1) dividing the basis function into two halves, 2) negating one-half of the basis function values, and then, 3) reversing the order of the basis function halves.

In conjunction with the original WDCS architecture, the BCASK data modulation proved to be very effective, producing bit error results consistent with orthogonal modulation and providing good interference suppression performance. The original WDCS implementation only considered binary modulation. Therefore, the proposed WDCS extends previous work to include *M-Ary* orthogonal signaling – the main impetus for the research being reported here.

2.3.1.5 System Timing.

The WDCS interference avoidance process is quite robust in both bursty and stable electromagnetic environments. This robustness is a result of many factors, including, 1) the WDCS samples the local electromagnetic environment in the time-domain to create communication basis functions, and 2) short sampling intervals decrease system sensitivity to electromagnetic environmental variation [2, 7, 9].

A simplified timing diagram is shown in Figure 6. The diagram shows the complete procedure for spectral sampling, basis function generation and processing, and waveform transmission, all of which occur over an interval dubbed the *frame time*,

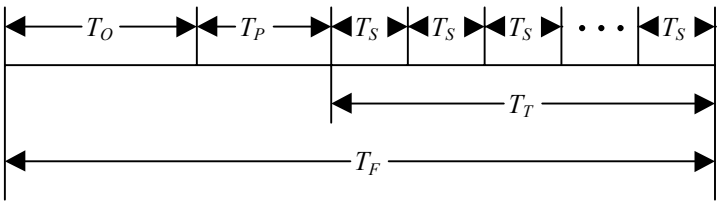

Figure 6. Timing Diagram [9].

denoted T_F. The *observation time*, T_O, is the time spent observing, or sampling, the electromagnetic environment. The sampling interval is an operationally dependent parameter and is not investigated as part of this research. The total time required to completely process the sampled data, including spectral estimation, thresholding, phase coding, scaling, and basis function generation is designated as *processing time*, T_P. Communication symbols are transmitted consistent with *a priori* criteria, including a set of M possible communication symbols each transmitted over identical, fixed time intervals called the *symbol time,* T_S. The *transmission time*, T_T, is the time spent transmitting communication symbols. At the end of each transmission interval, the process repeats [2, 7, 9]. Appropriate timing characteristics and intervals are primarily dependent on operational issues associated with system implementation. The focus of this research does not include dealing with such issues nor the optimization of timing parameters for system implementation.

Non-stationary interference sources present a unique challenge to the spectral estimation process. Any environmental changes occurring during the processing or transmission times may result in using a less efficient basis function for communicating, i.e., the basis function currently in use was generated from a previous spectral estimate containing different interference frequencies. In this case, an increased bit error rate, (P_b), is expected since the current basis function is not tailored to the current environment.

2.3.1.6 Previous WDCS Performance.

Previous WDCS performance was shown comparable to the original TDCS for all scenarios considered. Furthermore, the original WDCS provided an additional capability by accurately estimating a swept-tone interferer, a source of non-stationary interference. The previous metric for performance evaluation and comparison purposes was bit error rate (P_b). To validate proposed packet-based WDCS improvements, previous WDCS results are summarized in Table 1 and are referenced throughout the following chapters. All test scenarios considered in the original WDCS work are precisely replicated for this research to ensure accurate and valid performance characterization.

Table 1. Summary of Average WDCS Performance for BCASK [2, 12]

No Interference Present *Communication Performance* Variation from Bound	Interference Present and Avoidance Mechanisms Applied *Bit Error Rate Improvement*	
$\sim 10^{-3}$	Partial band and Swept-Tone	Single and Multiple-Tone
	6.6 dB	7.4 dB

2.4 Summary

This chapter provided relevant background information on previous TDCS and WDCS research, including discussions on fundamental processes common to both systems. The original WDCS architecture was provided in detail and two shortcomings identified to emphasize motivation for the current research, namely, 1) the original WDCS implementation could not effectively localize high frequency interference, and

2) the original WDCS implementation did not consider *M-Ary* orthogonal signaling applications. The chapter concludes with a summary of previous WDCS performance results.

3 Methodology

3.1 Introduction

This chapter introduces techniques implemented to model and simulate proposed Wavelet Domain Communication System (WDCS) performance. To simplify computer analysis and reduce simulation run time, lowpass complex envelope signal representation is used with Monte Carlo simulation techniques, as discussed in Section 3.2. Sections 3.3 through 3.5 provide details on the specific wavelet packet decomposition technique used for this work. The remainder of the chapter describes various implementations of the WDCS processes discussed in Chapter 2, as well as interference generation and model verification and validation techniques.

3.2 Computer Simulation Process

The lowpass complex envelope signal representation provides a valuable tool for simplifying computer modeling and simulation of WDCS performance. To satisfy Nyquist sampling criterion, i.e., to minimize adverse signal aliasing effects and allow reliable signal reconstruction, a signal must be sampled at twice the highest frequency of the signal [11]. Generally, the bandpass signal carrier frequency is much greater than the highest frequency component of the baseband information signal. Therefore, by separating the information-bearing signal from the modulating (carrier) signal, the

required sampling rate can be greatly reduced, providing a significant reduction in the amount of data required for effective simulation. The resultant decrease in computational requirements generally yields shorter simulation run times. The lowpass complex envelope signal representation is very versatile and can be used to represent both deterministic signals and Additive White Gaussian Noise (AWGN) [15]. Additionally, based on the equivalence theorem, this work assumes the specific spectral location of the communication signals is relatively unimportant and results can be readily extended to any spectral region [11].

The Monte Carlo method plays an equally important role in computer simulation of communication systems. The Monte Carlo method is fundamentally based on the implementation of a series of Bernoulli trials. In the case of digital communication systems, the total number of bit errors generated is divided by the total number of trials, yielding an estimate of bit error probability (P_b). If the communication symbols have equal probability of occurrence, the probability of bit error is given by (3) where n is the number of observed bit errors and N_t is the number of trials [16].

$$P_b \approx \lim_{N_t \to \infty} \frac{n(N_t)}{N_t} \tag{3}$$

$$P_b \approx \frac{n}{N_t} \tag{4}$$

By the strong law of large numbers, (3) converges to (4) as the number of trials approaches infinity [16]. Previous TDCS and WDCS research determined that approximately 500 trials are sufficient to provide convergence to within an acceptable

confidence interval. No optimality is implied by selecting 500 trials, rather, this number produces consistent results in a reasonably short processing time (number of trials vs. processing time tradeoff) [2].

3.3 Wavelet Packet Implementation

The newly proposed packet-based WDCS architecture is built on previously demonstrated WDCS technology [12] and is implemented in accordance with Figure 1. This previous WDCS architecture used conventional wavelet techniques and a Daubechies 8 mother wavelet [14, 17] for spectral estimation. For this work, no changes are made to the original WDCS architecture, i.e., the functionality of the shaded blocks in Figure 1 remains the same - only the internal wavelet spectral estimation mechanism is modified, i.e., the original Wavelet processing is replaced with a Wavelet packet decomposition technique.

3.4 Packet-Based Wavelet Spectral Estimation Process

For completeness, the following discussion of WDCS processing is provided. A Wavelet packet decomposition technique was introduced in this work to 1) increase transform adaptability over a larger class of interfering signals, 2) provide finer high-frequency resolution, and 3) permit implementation of *M-Ary* orthogonal signaling (not previously demonstrated). For this work, the Wavelet tree structure is effectively

expanded using a nonlinear, adaptive thresholding process, i.e., after initial Wavelet sub-band decomposition, the tree structure is expanded by splitting and down-sampling the lowpass *and* highpass wavelet branches of selected sub-bands, effectively providing finer resolution at higher frequencies when compared to a basic Wavelet decomposition technique [17].

3.4.1 Mother Wavelet.

As previously stated, the original WDCS architecture used conventional wavelet techniques and a Daubechies 8 mother wavelet [14, 17] for spectral estimation. However, the previous work made no claims of "optimality," rather, this particular wavelet technique was chosen since it possessed desirable properties of orthogonality, time-frequency localization, and multi-resolution; it was successfully exploited and clearly demonstrated the potential for using wavelet techniques to improve transform domain performance. Additional information on wavelet processing is provided in Section 2.3.1.

3.5 Threshold Determination

The adaptive thresholding and decomposition process of this work is outlined in Figure 7. After initial WDCS wavelet sub-band decomposition, the power in each sub-band (P_{Sub}) is compared to a threshold value (T) that is set according to the environmental noise power. If no P_{Sub} values exceed that of the noise by 20% (an empirically chosen threshold value providing acceptable results in previous work [12]), all coefficients are

retained (assigned a value of one) and a uniform "un-notched" spectral magnitude vector is passed on for subsequent phase coding and basis function generation (see the next paragraph). However, if P_{Sub} in *any* branch exceeds that of the noise by 20%, interference is declared present and an iterative sub-band decomposition process is applied to that branch. In this case, each branch with P_{Sub} exceeding the threshold is further decomposed per Figure 7 to enhance the interference time-frequency localization.

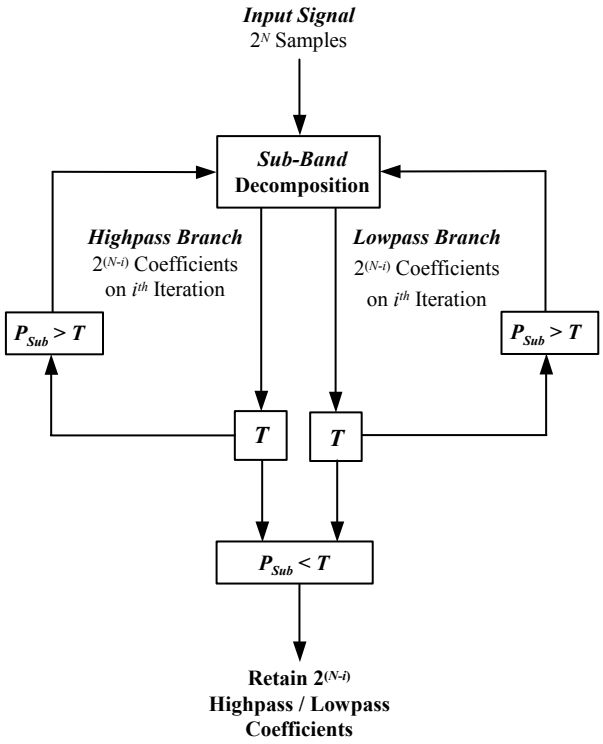

Figure 7. WDCS Sub-Band Thresholding and Decomposition Process.

The iterative thresholding and decomposition process repeats until one of two conditions occurs, namely, 1) the Wavelet tree structure has been fully expanded or, 2) the process is terminated per predetermined resolution criteria. Following iterative decomposition, a "notched" spectral magnitude vector is generated by setting the retained Wavelet sub-band coefficients to one and those exceeding the threshold to zero.

3.6 Phase Mapping / Encoding

Per Figure 1, a pseudo-random (PR) phase weighting is applied to each "notched" magnitude vector, creating a vector of complex elements having PR phase. Section 2.3.1.3 describes the phase mapping process in detail. The complex magnitude vector is then scaled and inverse Wavelet transformed to create the time-domain waveform, called a *basis function*. The resultant basis function waveform, (*b(t)*), is subsequently data modulated prior to transmission. Assuming the WDCS receiver remotely generates an identical (or nearly identical) basis function, the receiver uses the generated basis function to estimate communication symbols as done in a typical communication system, i.e., via matched filtering or correlation.

3.7 Basis Function Generation and Modulation

As a departing point from previous WDCS research, *M-Ary* orthogonal data modulation is considered exclusively for this research. Specifically, *M-Ary Cyclic Shift Keying* (MCSK) has been shown to represent a form of orthogonal signaling with TDCS implementations and is used here [8]. The MCSK notation $x((t - T/N))_T$ is introduced whereby each of the M communication symbols are represented by various circular shifts of $x(t)$ by one-N^{th} of symbol period T, i.e., $N = 1, 2, 3, \ldots M$ - the notation used in (5) to illustrate 4-*Ary* CSK.

$$
\begin{aligned}
s_1(t) &= b(t) \quad \text{(Basis Function)} \\
s_2(t) &= b\left(\left(t-\frac{T}{4}\right)\right)_T \\
s_3(t) &= b\left(\left(t-\frac{T}{2}\right)\right)_T \\
s_4(t) &= b\left(\left(t-\frac{3T}{4}\right)\right)_T
\end{aligned}
\tag{5}
$$

The theoretical symbol error probability, P_M, for coherently detected *M-Ary* orthogonal signaling over an AWGN channel is well established and is given by (6), where E_S is the average energy per symbol, k is the number of bits per symbol, N_0 is the noise power spectral density, and the *Q(x) function*, as expressed in (7), is derived from the Complementary Error Function [18].

$$
P_M \le (M-1)Q\left(\sqrt{\frac{E_S}{N_0}}\right) \quad \begin{cases} \text{M-Ary Orthogonal} \\ M = 2^k,\ E_S = kE_b \end{cases} \tag{6}
$$

$$
Q(x) = \int_x^{\infty} \frac{1}{\sqrt{2\pi}} e^{-\frac{z^2}{2}} dz \tag{7}
$$

For equiprobable orthogonal signaling, P_M may be easily converted to average bit error probability P_b using (8). Thus a theoretical upper bound on communication performance bit error probability P_b can be derived from (6) and (8) and is given by (9).

$$
P_b = \frac{2^{k-1}}{2^k - 1} P_M = \frac{M/2}{M-1} P_M \tag{8}
$$

$$P_b \le 2^{k-1} Q\left(\sqrt{\frac{k E_b}{N_o}}\right) \tag{9}$$

A set of M equal energy signals forms an orthonormal set if, and only if, (10) is satisfied for $i,j = 1, 2, 3,\ldots M$, and $\alpha_{ij} = 0$. If $\alpha_{ij} << 1$, the signals can be considered "quasi-orthogonal" and are still effective in communication applications. As mentioned above, *M-Ary* CSK represents a form of orthogonal signaling, i.e., the set of M communication symbols satisfy (10). Generally, communication signals (symbols) are *less* orthogonal as the magnitude of α_{ij} *increases* and overall system performance is degraded, i.e., P_b increases. Note that in the *binary signaling* case, two signals can be chosen such that α_{ij} is negative and the signaling scheme is no longer classified as orthogonal, e.g., when α_{ij} approaches –1 the signals represent a from of antipodal signaling [11].

$$\rho_{ij} = \frac{1}{E_b}\int_0^T s_i(t)s_j(t)dt = \begin{cases} 1 & i = j \\ \alpha_{ij} & i \ne j \end{cases} \quad -1 \le \rho_{ij}, \alpha_{ij} \le 1 \tag{10}$$

The remainder of this section applies for equal-energy *binary* signaling over an AWGN channel using coherent detection. The effect of signal cross-correlation on bit error performance is seen in (11), where the normalized cross-correlation coefficient between the two signals, ρ, is defined by (10) [11].

$$P_b = Q\left(\sqrt{\frac{E_b(1-\rho)}{N_0}}\right) \tag{11}$$

Using signal space concepts, the binary cross-correlation coefficient can also be calculated per (12) where θ is the angular separation between the signals, as illustrated in Figure 8 [11]. From (11), it is evident that as ρ approaches a value of –1 (equivalent to θ approaching π radians) binary bit error performance becomes optimal, as in the case of antipodal binary signaling. For orthogonal binary signaling, $\rho = 0$ ($\theta = \pi/2$ radians), bit error performance is poorer than the optimal antipodal case. Bit error variation due to variations in the correlation coefficient are illustrated in Figure 9 for $\rho = 0$ and $\rho = 0.6$.

$$\rho = \cos\theta \quad -1 \le \rho \le 1 \tag{12}$$

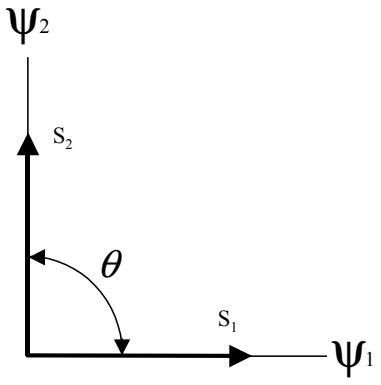

Figure 8. Binary Signaling: Signal Space Representation [11].

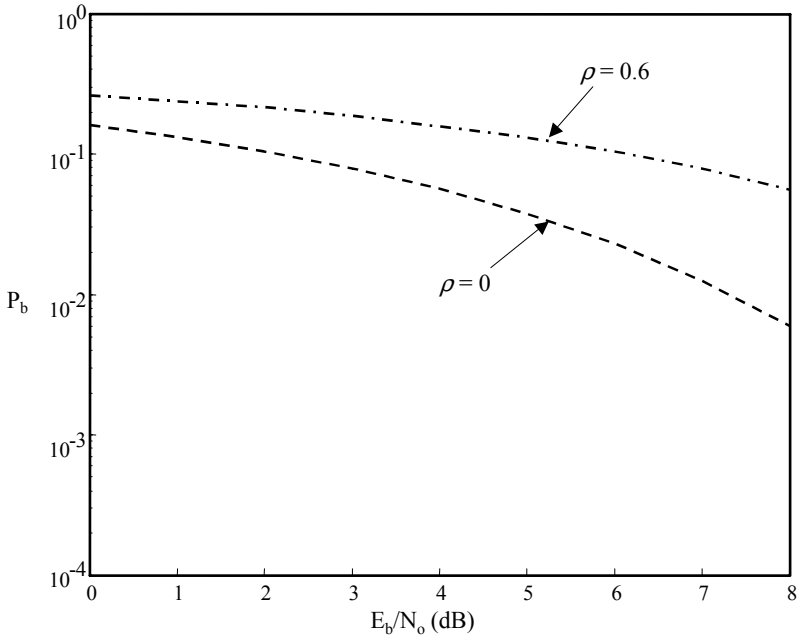

Figure 9. Binary Signaling: Cross-Correlation Effects.

3.8 Interference Models

The five interference models developed for this work were based on previous WDCS and TDCS research - no changes were made to the original models [1, 2]. As such, information in this section is provided for completeness and derived from [1, 2]. The interference models are implemented using the lowpass complex envelope signal representation as outlined in Section 3.2. All interference realizations contain the same total average power for a given interference energy-to-signal energy ratio (*I/E*). Each simulation trial generates a new, uncorrelated realization of the interference under consideration.

3.8.1 Partial Band Interference.

The 10% and 70% partial band interference is generated in the frequency domain via the Fourier transform. First, an interference magnitude vector is created having the desired relative spectral width, e.g., for 10% partial band interference 10% of the interference magnitude vector elements are set to one and the remaining 90% are set to zero. The interference magnitude vector is then multiplied, element-by-element, with a weighted pseudo-random (PR) vector to achieve the desired *I/E* ratio and induce PR phase. An inverse Fourier transform is then applied to the complex interference vector to generate the time domain representation of the interference signal.

3.8.2 Swept-Tone Interference.

To effectively model the swept-tone interference it is necessary to place constraints and limits on the number of degrees-of-freedom. The following constraints are enforced, namely the interferer:

1. operates totally within the WDCS bandwidth during the sweep time.
2. occupies 60% of the total WDCS system bandwidth.
3. completes only *one* sweep during the observation time, T_O. This represents a 'best case' scenario from a spectral estimation standpoint and allows the estimation process to effectively estimate the interference.
4. completes *one* sweep in an interval equal to *five* symbol times (T_S).

The swept-tone interference is modeled as a complex sinusoid having a random starting phase. The amplitude of the sinusoid is scaled to achieve the desired *I/E* ratio.

3.8.3 Single and Multiple-Tone Interference.

Similar to the swept-tone interference, the single and multiple-tone interferers are modeled as complex sinusoids having random starting phases. The single tone interference energy is controlled by appropriately scaling a single-frequency sinusoid. The multiple-tone interference represents a summation of seven single-frequency sinusoids, each having distinct, random starting phases. The amplitude scaling is applied to the tones such that each tone contains one-seventh of the desired energy level.

3.9 WDCS Model Verification and Validation

As described in Section 3.2 a Monte Carlo simulation method is implemented and used to perform WDCS model verification and validation. Using MATLAB®, simulated *communication performance* (no interference present) is characterized for average signal bit energy-to-noise power spectral density (PSD) levels (E_b/N_0) ranging from 0.0 dB to 8.0 dB and compared with analytic results of (9), as derived in Section 3.7. WDCS *suppression performance* (interference present) is simulated using an E_b/N_0 value of 4.0 dB and average interference-to-average signal energy (I/E) levels ranging from 0.0 dB to 16.0 dB. All simulated scenarios are run for binary, 4-*Ary*, and 8-*Ary* CSK data modulations. Performance characteristics for binary signaling are compared to previous WDCS results as summarized in Table 1 of Section 2.3.1.6.

3.10 Summary

This chapter begins by describing the methods used to accurately and efficiently model and simulate performance of the proposed packet-based WDCS architecture; a lowpass complex envelope signal representation is used with Monte Carlo simulation techniques. Next, specific details of the Wavelet packet decomposition implementation and thresholding process are outlined as they apply to spectral estimation and basis function generation. A discussion of Cyclic Shift Keying (CSK) follows, including necessary conditions defining orthogonality and the impact of cross-correlation on degraded bit error performance. Next, the interference models are introduced and the implementation of each is discussed. Finally, the verification and validation processes for the proposed packet-based WDCS are provided.

4 Simulation Results and Analysis

4.1 Introduction

This chapter begins by characterizing the WDCS basis function and analyzing communication symbol cross-correlation characteristics, as affected by increased interference energy. To effectively employ orthogonal Cyclic Shift Keying (CSK) data modulation, it is desirable that the basis function exhibits and adheres to specific properties as presented in Section 4.2. Communication symbol cross-correlation properties are characterized as a function of interference-to-average signal energy (*I/E*) levels ranging from 0.0 dB to 16.0 dB. Section 4.3 provides illustrative Wavelet domain representations, as obtained via the wavelet packet decomposition process outlined in Sections 3.3 - 3.5, for all interferers considered under this work. In Section 4.4, simulated *communication performance* (no interference present) is presented for average signal bit energy-to-noise power spectral density (PSD) levels (E_b/N_0) ranging from 0.0 dB to 8.0 dB and compared with analytic results of (9), as derived in Section 3.7. Section 4.5 presents WDCS *suppression performance* (interference present) and sensitivity analyses for an E_b/N_0 value of 4.0 dB and (*I/E*) levels ranging from 0.0 dB to 16.0 dB. Simulation results are provided for all interference scenarios using binary, 4-*Ary*, and 8-*Ary* CSK data modulations. The chapter concludes with a series of tables summarizing WDCS performance and includes a comparison of the proposed packet-based WDCS performance with original WDCS results.

4.2 Basis Function / Communication Symbol Characteristics

The phase distribution and autocorrelation response of a representative WDCS basis function (*b(t)*) are shown in Figure 10 and Figure 11, respectively. The basis function exhibits desirable correlation properties that make it possible to implement *M-Ary* CSK data modulation, i.e., 1) *b(t)* is orthogonal (at least quasi-orthogonal) to cyclic shifts of itself and 2) the autocorrelation response has a normalized peak sidelobe level of minus 10.1 dB.

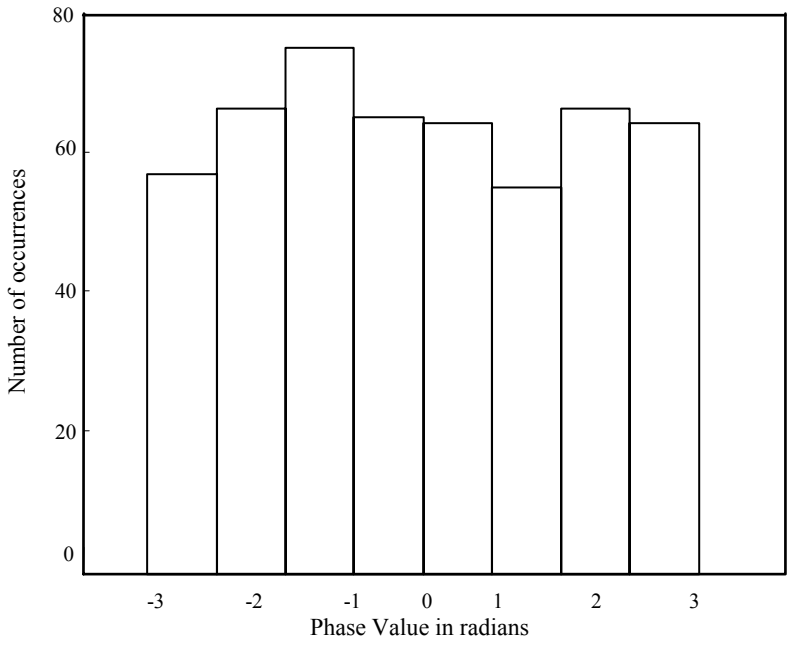

Figure 10. WDCS Basis Function Phase Distribution.

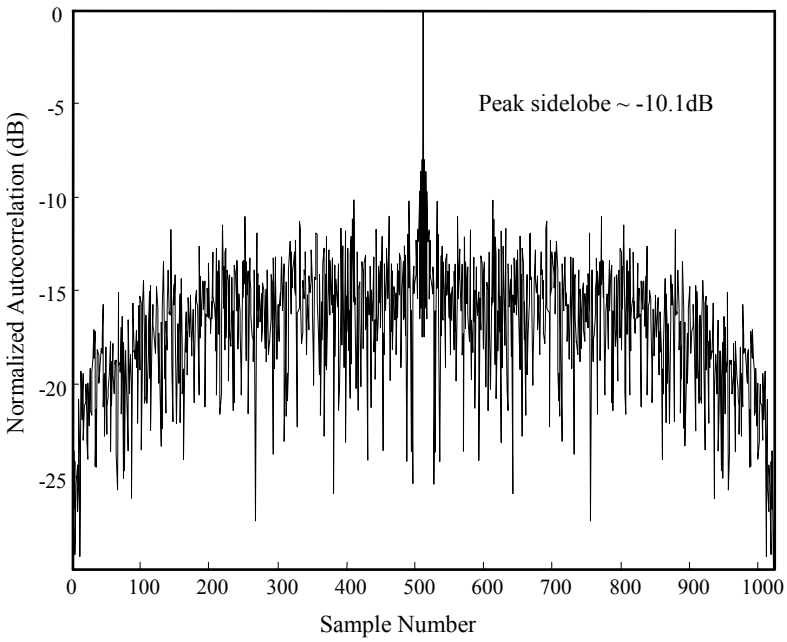

Figure 11. WDCS Basis Function Autocorrelation.

One fundamental cause of performance degradation in communication systems is increased symbol cross-correlation; in orthogonal signaling schemes, this is analogous to loss of symbol orthogonality. Figure 12 shows average symbol cross-correlation for *M-Ary* CSK as a function of increasing interference-to-average signal energy (*I/E*) levels for 10% partial band interference with *interference avoidance mechanisms applied*. The 10% partial band interference was selected since it represents a 'worst case' interference source for the WDCS, producing the largest increase in bit error rate (P_b) for binary, 4-*Ary*, and 8-*Ary* modulations (See Section 4.5). As shown in Figure 12 average communication symbol cross-correlation generally follows an upward trend as *I/E* increases. Based on this trend, the expectation is that communication performance will suffer (P_b will increase) at higher levels of *I/E* for partial band interference scenarios.

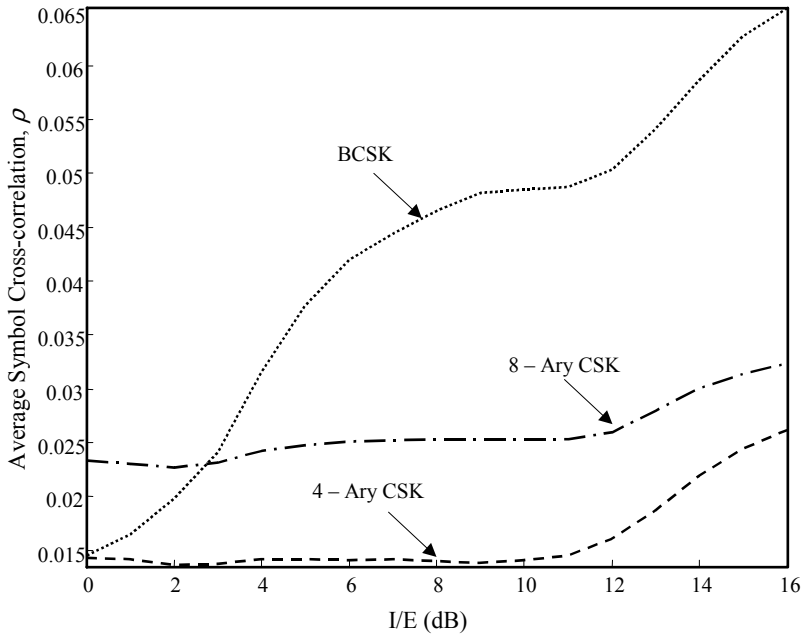

Figure 12. WDCS Communication Symbol Cross-Correlation. 10% Partial Band Interference

Section 3.7 provided an analytic expression for cross-correlation effects on binary orthogonal signaling, validating the adverse effects of increased symbol cross-correlation on communication performance (See Figure 9). Although the cross-correlation effects discussed above do not fully account for all performance degradation experienced, it is one of two causes identified in this work.

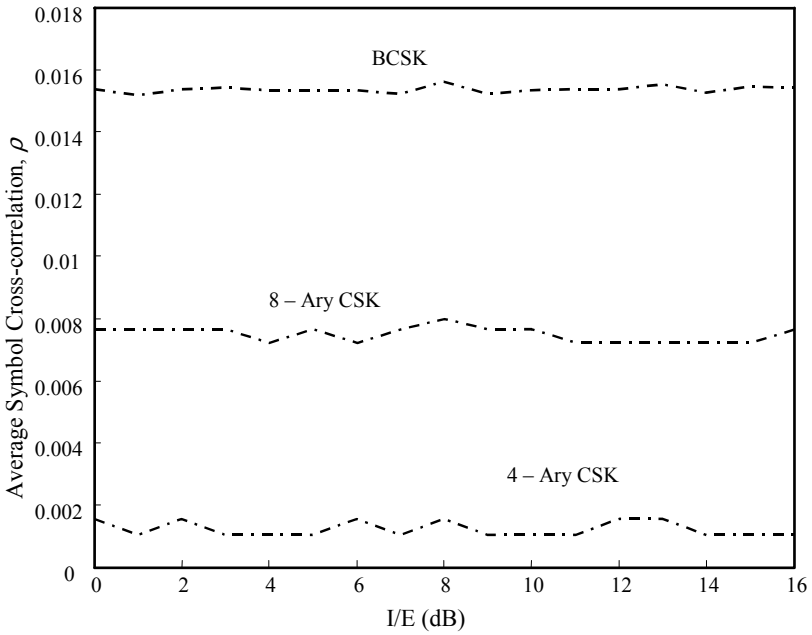

Figure 13. WDCS Communication Symbol Cross-correlation. Single-tone interference

In contrast to the cross-correlation effects seen in the partial band interference case, Figure 13 was generated in the same fashion as Figure 12, but for a single-tone interference scenario. As shown for the sinusoidal tone interference scenario, symbol cross-correlation does not exhibit the same upward trend as the partial band interference case. Furthermore, the average symbol cross-correlation values, ρ, are much lower than the previous case. Based on this observation, it is anticipated that there will be minimal performance degradation. Section 4.3 discusses this interesting behavior in more detail.

4.3 Wavelet Packet Decomposition of Various Interference Sources

The following wavelet packet decompositions are presented to demonstrate the high frequency resolution achieved by the packet-based WDCS decomposition process, as well as to illustrate wavelet packet representations for the different interference sources considered (Figure 14 through Figure 20). Each figure (except for Figure 14 and Figure 16) was produced using an E_b/N_0 of 4.0 dB and an *I/E* value of 10.0 dB. The top plot in each figure (except for Figure 14 and Figure 16) represents the interference only case; the bottom plot represents the transform for the case including interference plus AWGN channel effects.

The representative partial band decompositions also serve to illustrate a second cause of increased bit error rate (P_b) identified in this work, namely, the interference energy that is *not* completely nulled out (notched) during basis function generation due to the fixed threshold value (set at 20% above the noise power). In Figure 14 (*I/E* of 0.0 dB), an interference region *not* exceeding the threshold (circled) is *not* nulled out during basis function generation. The same interference region is circled in Figure 15 (*I/E* of 10.0 db). There are additional regions of interference not exceeding the threshold, but only one is addressed here as a representative example. Figure 16 is an expanded view of the circled sections of Figure 14 and Figure 15 and illustrates the phenomenon for 10% partial band interference. As shown, the seemingly negligible regions of interference become an increasingly large factor as *I/E* increases, i.e., the interference

energy contained in the un-notched spectral regions steadily increases, corresponding to a steady decrease in P_b performance. Results presented in Section 4.5.1 clearly indicate this trend.

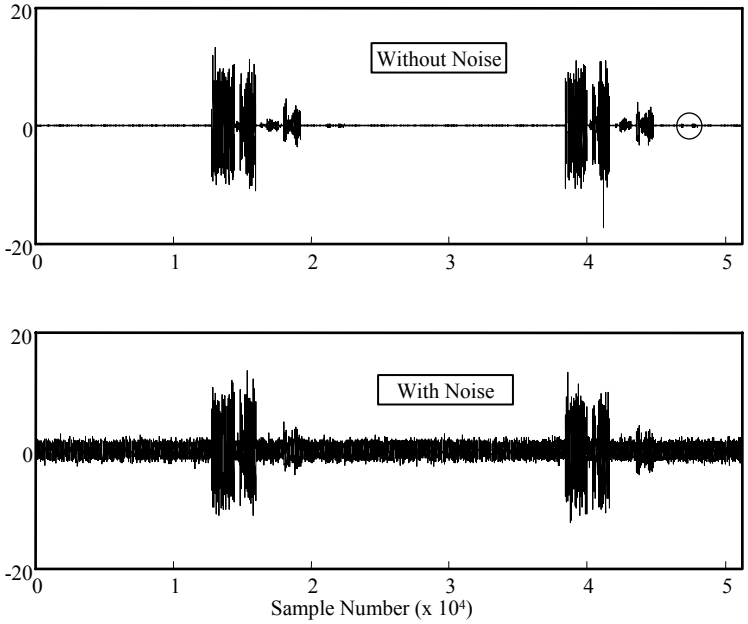

Figure 14. Wavelet Packet Transform: 10% Partial Band Interference with E_b/N_0 = 4.0 dB and I/E = 0.0 dB. Without AWGN (Top) and With AWGN (Bottom)

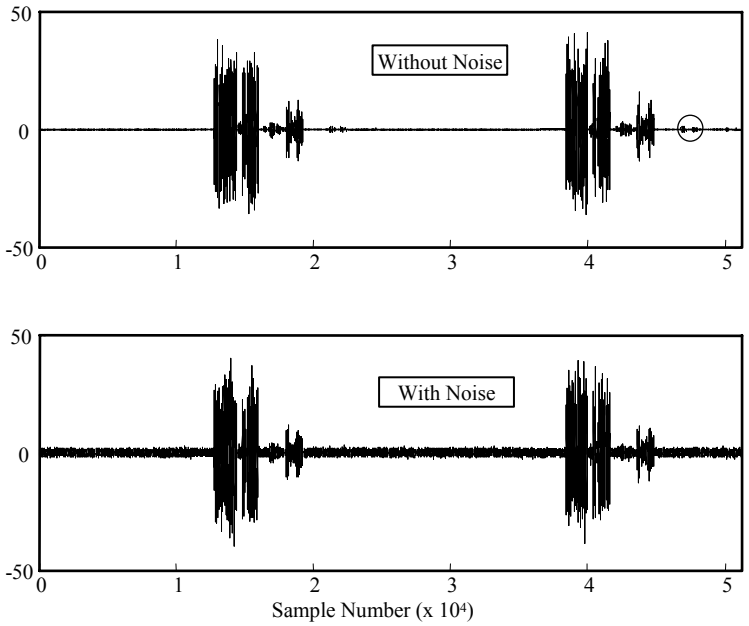

Figure 15. Wavelet Packet Transform: 10% Partial Band Interference with E_b/N_0 = 4.0 dB and I/E = 10.0 dB. Without AWGN (Top) and With AWGN (Bottom)

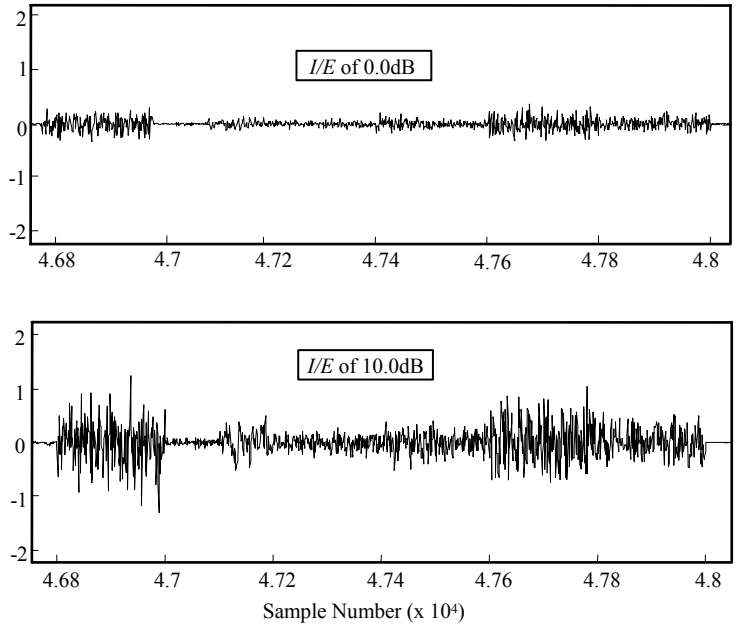

Figure 16. Wavelet Packet Transform: Expanded view, 10% Partial Band Interference with E_b/N_0 = 4.0 dB. I/E = 0.0 dB (Top) and I/E = 10.0 dB (Bottom)

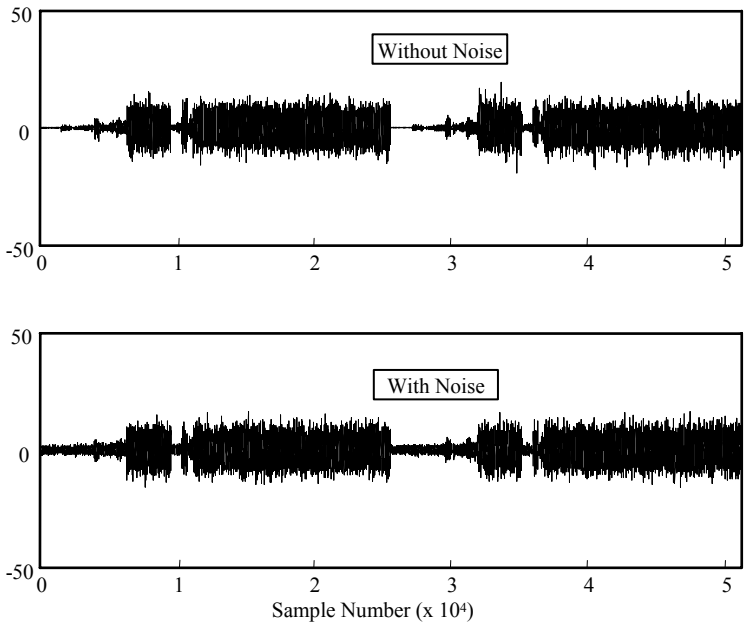

Figure 17. Wavelet Packet Transform: 70% Partial Band Interference with E_b/N_0 = 4.0 dB and I/E = 10.0 dB. Without AWGN (Top) and With AWGN (Bottom)

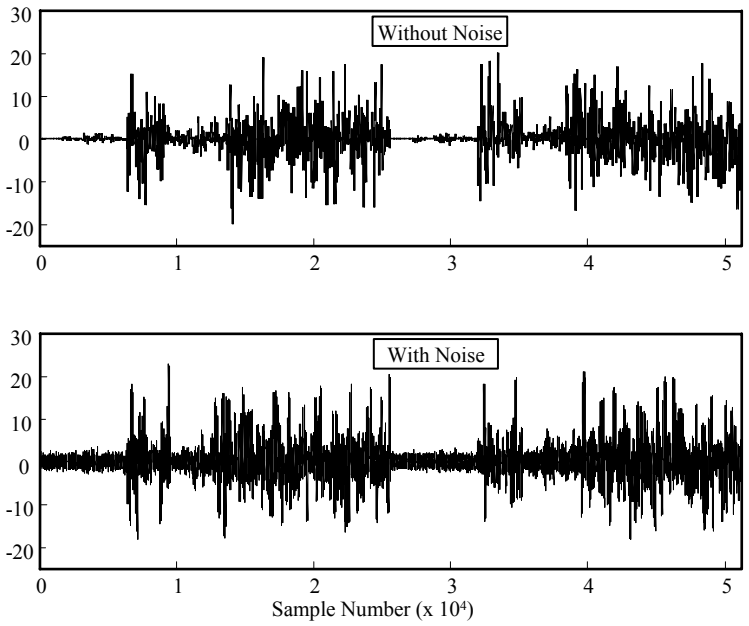

Figure 18. Wavelet Packet Transform: Swept-Tone Interference with E_b/N_0 = 4.0 dB and I/E = 10.0 dB. Without AWGN (Top) and With AWGN (Bottom)

In contrast to the partial band interference case, the single-tone and multiple-tone interferers spectrally focus all their energy at discrete locations. Consequently, these interference sources are more effectively avoided and have little impact on system performance, i.e., there are no un-notched spectral regions containing interference energy and the previously described phenomenon is not seen.

However, a second interesting phenomenon was observed and is worth noting, namely, the adaptive wavelet packet decomposition and thresholding process generates a basis function *with interference present* that has better correlation properties than a basis function generated without interference present. In this case, the resultant set of M symbols exhibits better cross-correlation properties and therefore produces better (lower) bit error rates, P_b, than simulated performance achieved with no interference present. This is clearly seen in the tone and multiple-tone simulation results presented in Section 4.5.2.

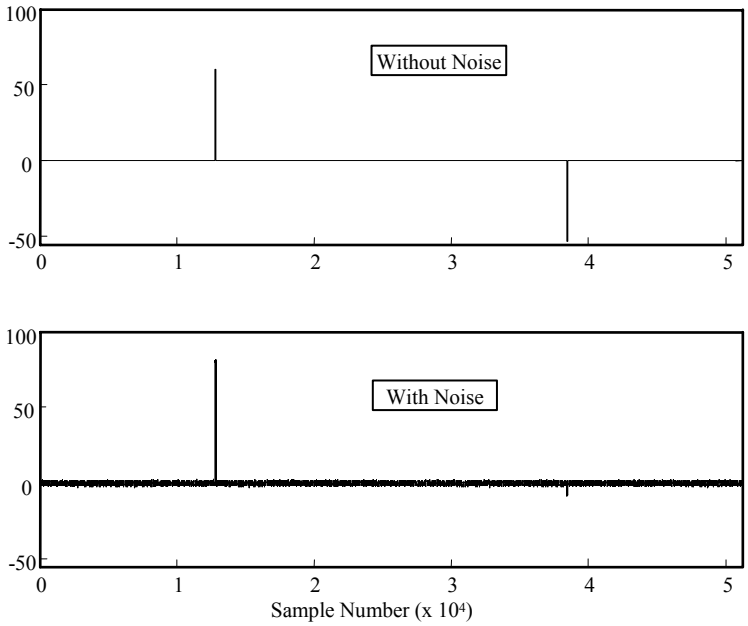

Figure 19. Wavelet Packet Transform: Single-Tone Interference with E_b/N_0 = 4.0 dB and I/E = 10.0 dB. Without AWGN (Top) and With AWGN (Bottom)

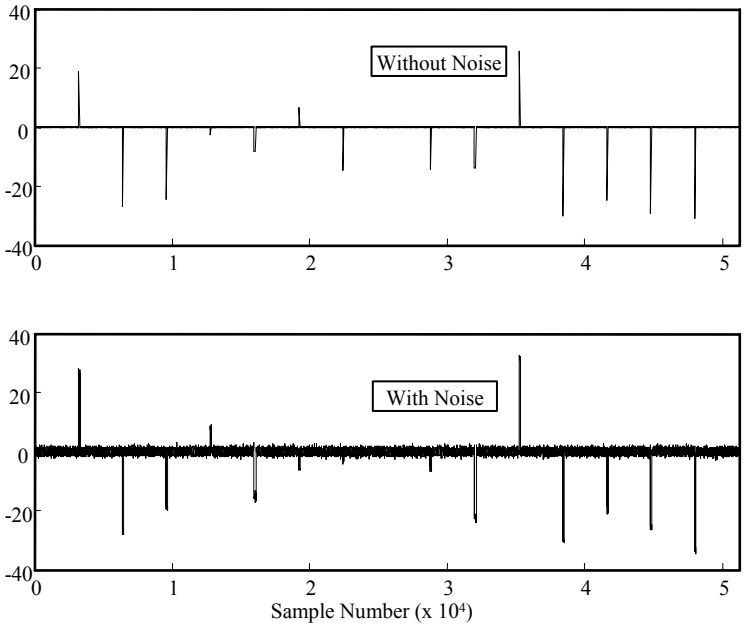

Figure 20. Wavelet Packet Transform: Multiple-Tone Interference with E_b/N_0 = 4.0 dB and I/E = 10.0 dB. Without AWGN (Top) and With AWGN (Bottom)

4.4 Model Verification and Validation – No Interference Present

Consistent with the previous WDCS validation processes, simulations were run for all models in the *absence* of interference to establish communication performance – obviously, the proposed technique is of minimal use if it cannot perform effectively and communicate in benign environments. Following communication performance validation, simulations were run for all scenarios with *interference present* to characterize *interference avoidance* capability (Section 4.5).

As shown in Figure 21, simulated communication performance (bit error rate) for the proposed packet-based WDCS (dashed line), for binary, 4-*Ary*, and 8-*Ary* CSK data modulations, is consistent with the theoretical upper bound (solid line) of (6) – the data reflect a mean delta (between theoretical and simulation) of 7.9×10^{-3} and standard deviation of 1.1×10^{-2} over the range of indicated E_b/N_0 values. Three values taken from the intersection of *simulated* communication performances and the dashed arrow reflected in Figure 21 for $E_b/N_0 = 4.0$ dB are designated as '*Communication Performance*' references. Represented by the constant dashed lines in subsequent interference avoidance analyses, these lines serve as a reference to provide a metric on how effective the proposed packet-based WDCS interference avoidance is.

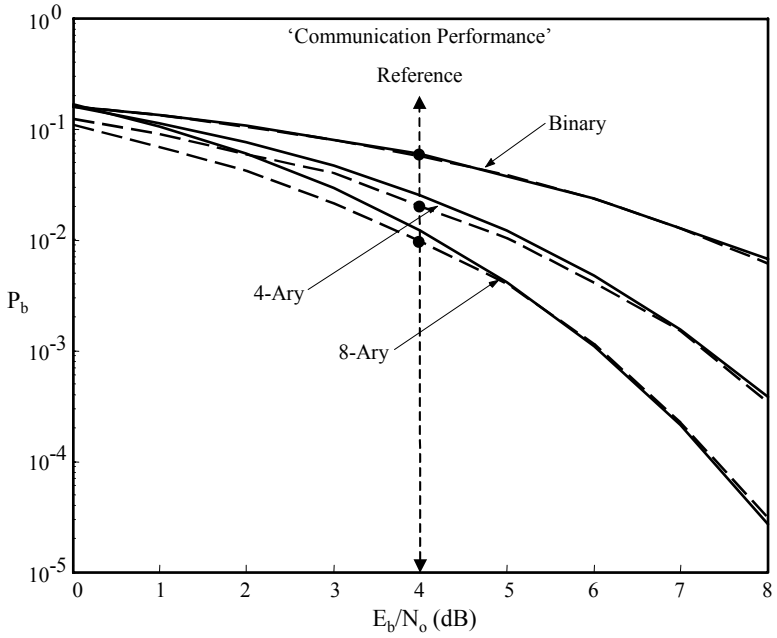

Figure 21. Packet-Based WDCS M-Ary Communication Performance No Interference Present [19].

4.5 Performance Characterization – Interference Present

Packet-based WDCS simulated performance was verified against theoretical performance for scenarios containing interference under two conditions, including scenarios with 1) no suppression mechanisms applied, i.e., no wavelet detail thresholding / nulling, and 2) suppression mechanisms employed. For all interference scenarios, the performance is evaluated while maintaining a constant E_b/N_0 of 4.0 dB and interference-to-average signal energy (I/E) levels ranging from 0.0 dB to 16.0 dB. For comparison, the theoretical performance is estimated by assuming constant interference power spectral density over the system bandwidth, effectively adding to the system noise floor and impacting symbol error performance of (6). Clearly, this is not a valid

assumption for the tone and narrow-band interference cases, but it does provide a means for bounding the analysis.

Additionally, WDCS bit error 'sensitivity' is examined for geographically separated and uncorrelated electromagnetic environments, i.e., the transceivers observe different environmental characteristics during the spectral sampling and estimation process.

4.5.1 Partial Band and Swept-Tone Interference.

This section is developed from the work presented in [19]. Figure 22 shows interference avoidance results for binary CSK using swept-tone and partial band interference (10% and 70%). As outlined in Section 4.4, the constant dashed line in the figure (and each subsequent figure) represents the *simulated* 'Communication Performance' taken from Figure 21 (no interference present) using a fixed E_b/N_0 of 4.0 dB. The communication performance is estimated by assuming constant interference power spectral density over the system bandwidth, effectively adding to the system noise floor and affecting symbol error performance of (6). Clearly, this is not a valid assumption for the tone and narrowband interference cases, and simulated results are expected to vary from estimated performance. Data in Figure 23 correspond to the average bit error performance for all interference scenarios considered in Figure 22 – in this case, there is an indicated interference avoidance capability and improvement of approximately 6.7 dB over the range of I/E values considered.

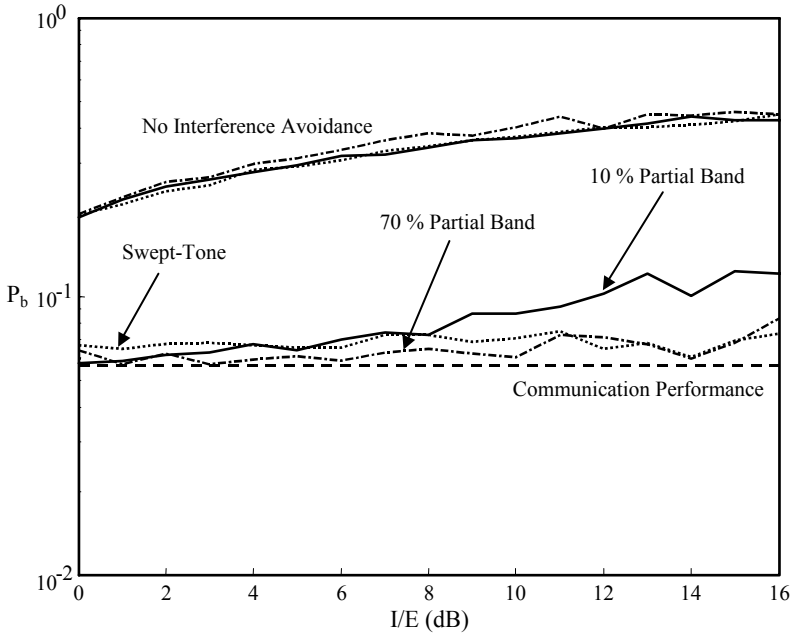

Figure 22. Binary Interference Avoidance: Swept-tone and Partial Band Interference (10% and 70%) [19].

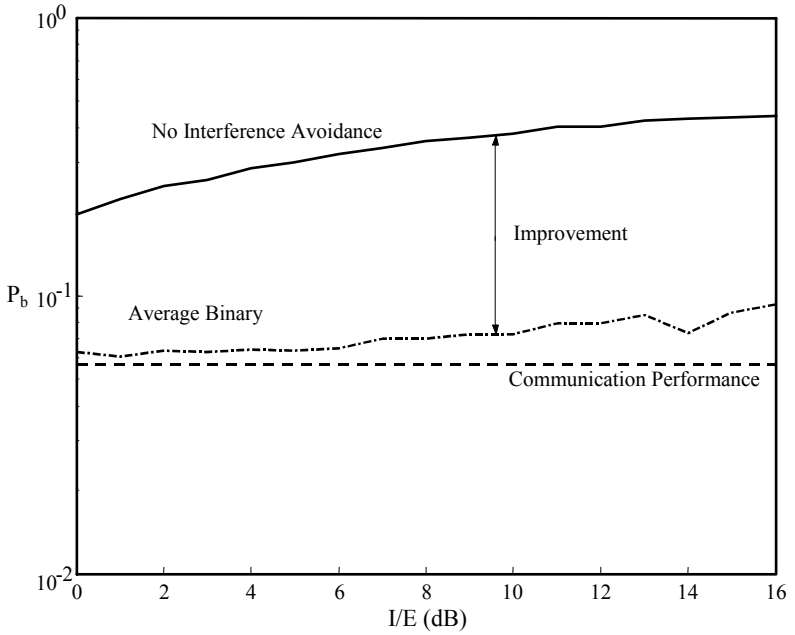

Figure 23. Average Bit Error: Binary CSK Modulation Swept-tone and Partial Band Interference (10% and 70%) [19].

Figure 24 shows interference avoidance results for 4-*Ary* CSK using swept-tone and partial band interference (10% and 70%). Figure 25 data represent the average bit error performance for all interference scenarios considered in Figure 24 – in this case, there is a demonstrated interference avoidance capability and improvement of approximately 9.2 dB over the range of *I*/*E* values considered.

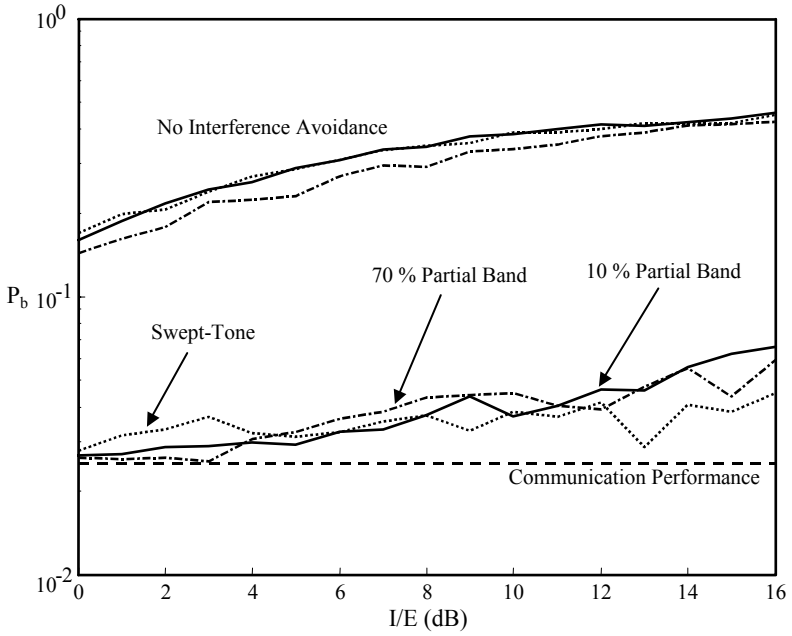

Figure 24. 4-Ary Interference Avoidance: Swept-tone and Partial Band Interference (10% and 70%) [19].

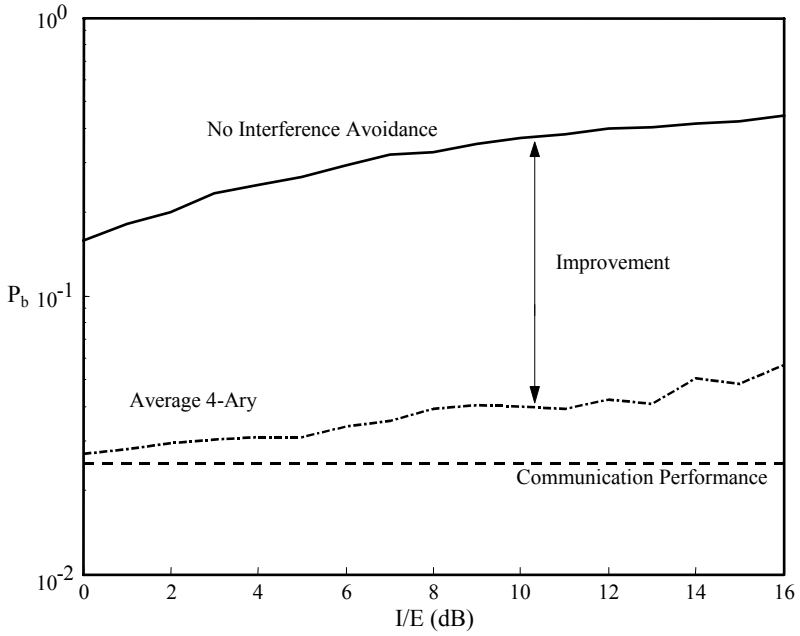

Figure 25. Average Bit Error: 4-Ary CSK Modulation Swept-tone and Partial Band Interference (10% and 70%) [19].

Figure 26 shows interference avoidance results for 8-*Ary* CSK using swept-tone and partial band interference (10% and 70%). Figure 27 data represent the average bit error performance for all interference scenarios considered in Figure 26 – in this case, there is a demonstrated interference avoidance capability and improvement of approximately 12.0 dB over the range of *I*/*E* values considered.

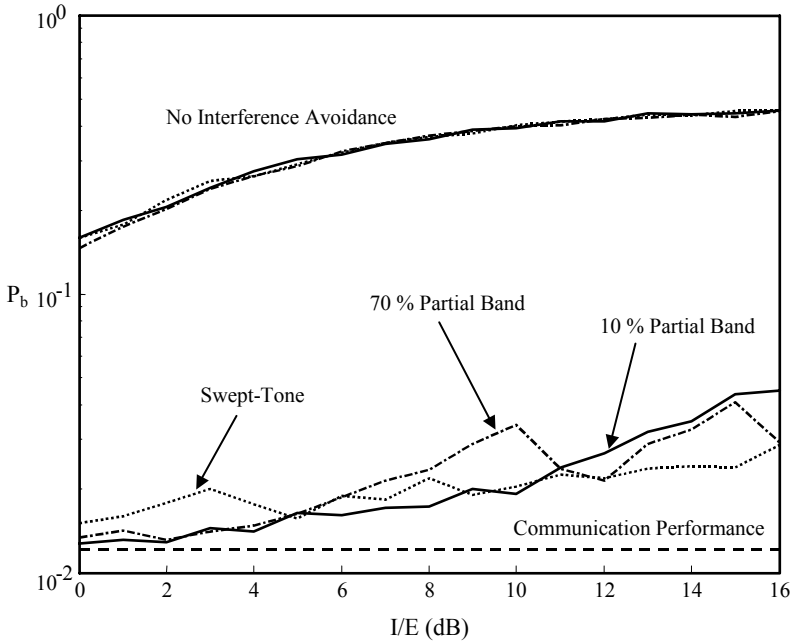

Figure 26. 8-Ary Interference Avoidance: Swept-tone and Partial Band Interference (10% and 70%) [19].

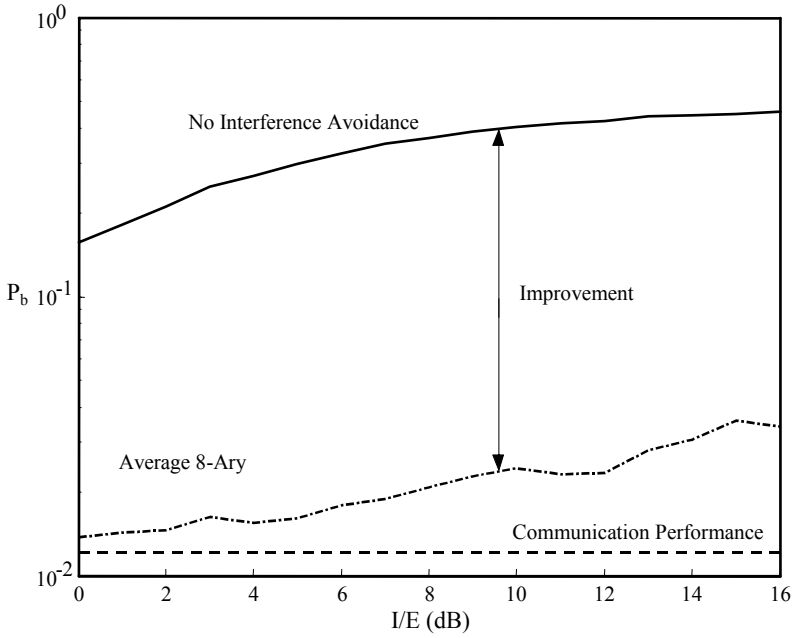

Figure 27. Average Bit Error: 8-Ary CSK Modulation Swept-tone and Partial Band Interference (10% and 70%) [19].

4.5.2 Single and Multiple-Tone Interference.

Figure 28 shows interference avoidance results for binary CSK using single and multiple-tone interference. Figure 29 data correspond to the average bit error performance for all interference scenarios considered in Figure 28 – in this case, there is an indicated interference avoidance capability and improvement of approximately 8.0 dB over the range of I/E values considered.

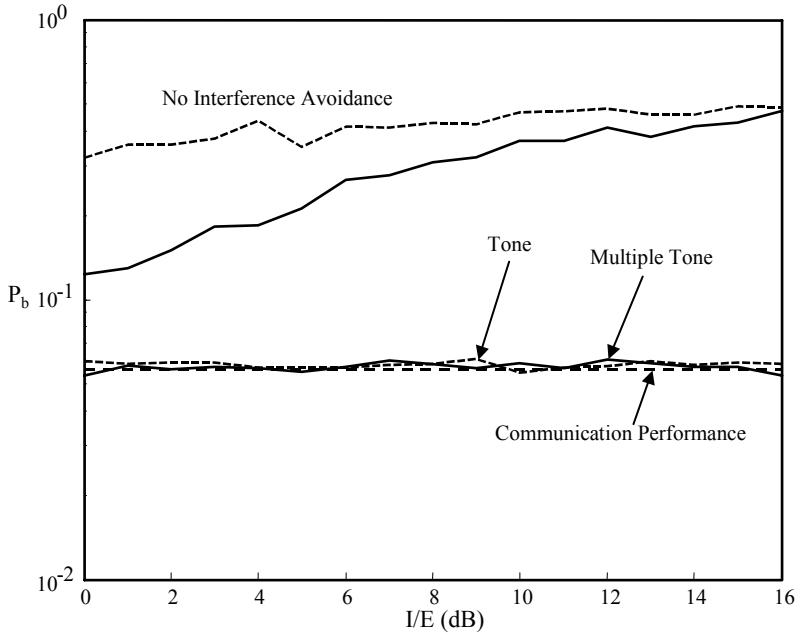

Figure 28. Binary Interference Avoidance: Single and Multiple-tone Interference.

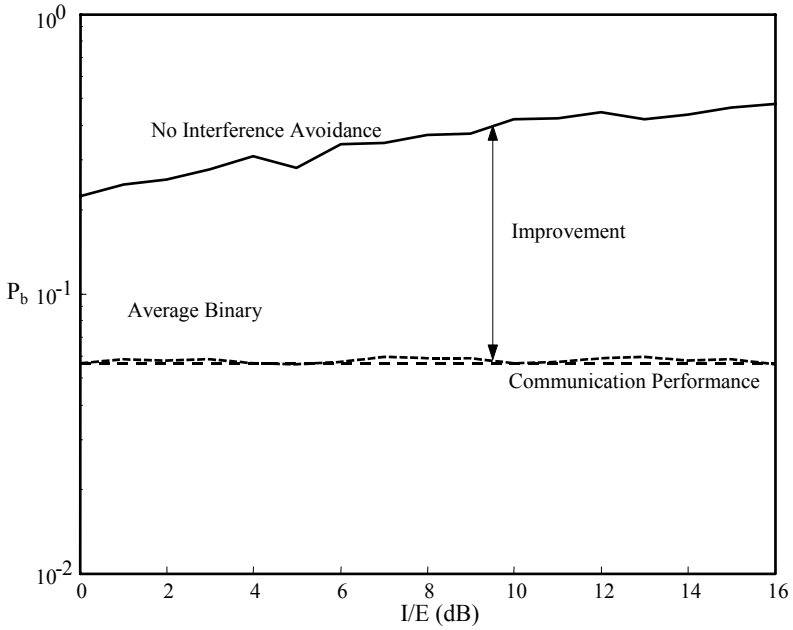

Figure 29. Average Bit Error: Binary CSK Modulation Single and Multiple-tone Interference.

Figure 30 shows interference avoidance results for 4-*Ary* CSK using single and multiple-tone interference. Figure 32 data represent the average bit error performance for all interference scenarios considered in Figure 30 – in this case, there is a demonstrated interference avoidance capability and improvement of approximately 12.4 dB over the range of *I*/*E* values considered.

An interesting anomaly begins to appear in the 4-Ary results of Figure 30 (as well as the subsequent data plots provided for 8-Ary CSK modulation), namely, the indicated bit error performance with interference present and avoidance mechanisms applied is better (lower) than the communication performance (dashed reference line) with no interference present. How can the WDCS achieve better bit error performance in an environment containing interference than one void of interference? An investigation into the correlation properties of the communication symbols, as generated from basis

functions for the two scenarios, revealed that the communication symbols for the interference scenario actually exhibit better (lower) average cross-correlation characteristics (Figure 31). As detailed in Section 3.7, better cross-correlation characteristics yield improved symbol estimation and better bit error performance.

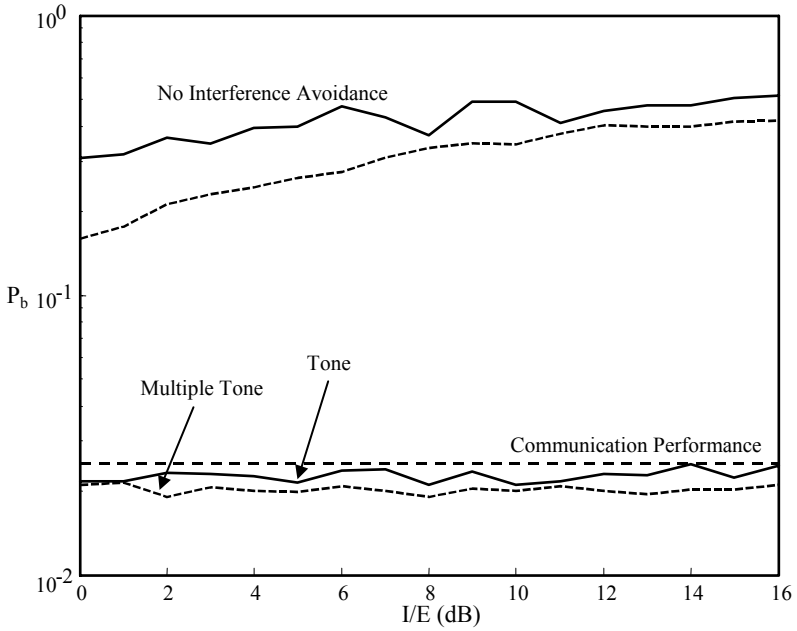

Figure 30. 4-Ary Interference Avoidance: Single and Multiple-tone Interference.

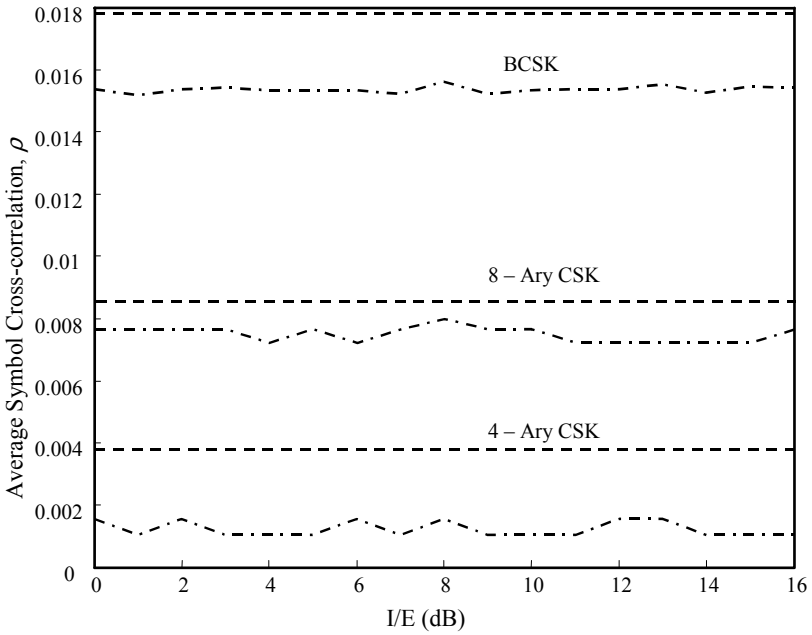

Figure 31. WDCS Communication Symbol Cross-Correlation. Single-Tone and No Interference (constant dashed lines).

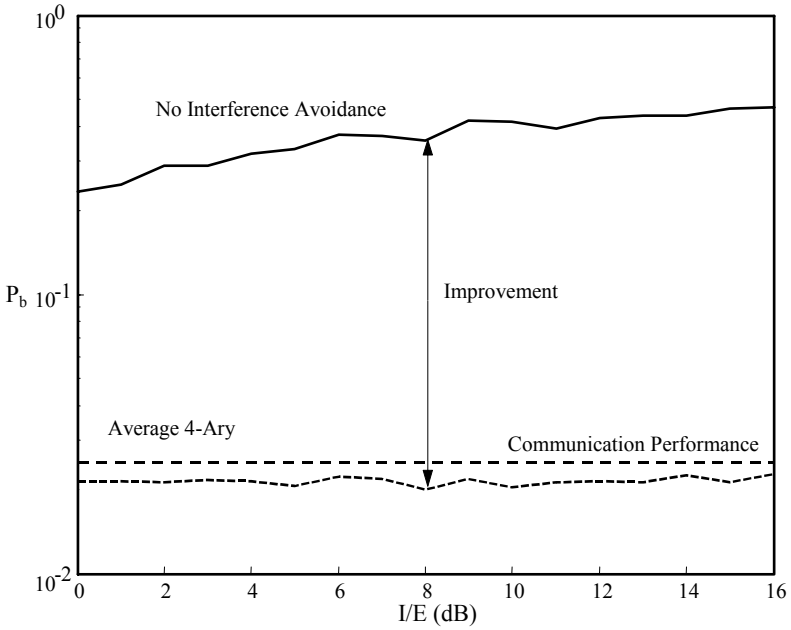

Figure 32. Average Bit Error: 4-Ary CSK Modulation Single and Multiple-tone Interference.

Figure 33 shows interference avoidance results for 8-*Ary* CSK using single and multiple-tone interference. Figure 34 data represent the average bit error performance for all interference scenarios considered in Figure 33 – in this case, there is a demonstrated interference avoidance capability and improvement of approximately 15.7 dB over the range of *I*/*E* values considered.

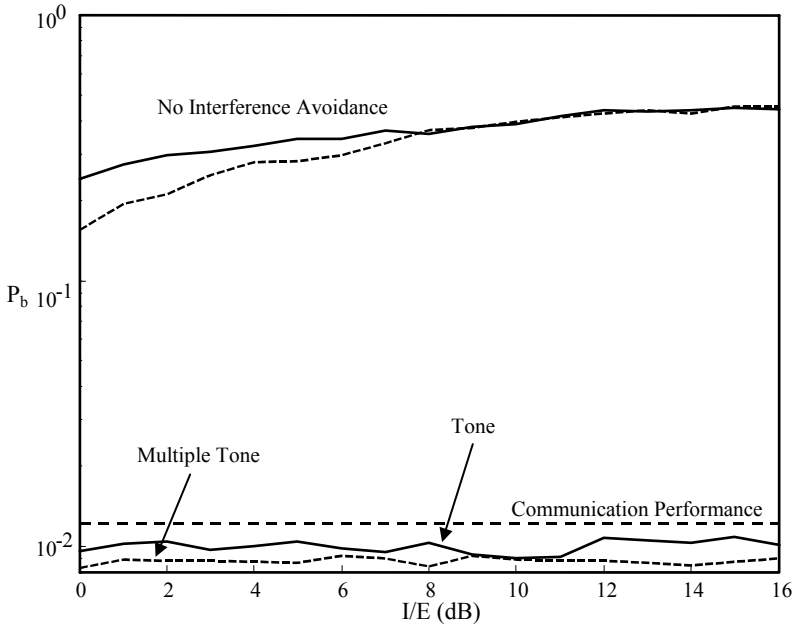

Figure 33. 8-Ary Interference Avoidance: Single and Multiple-tone Interference.

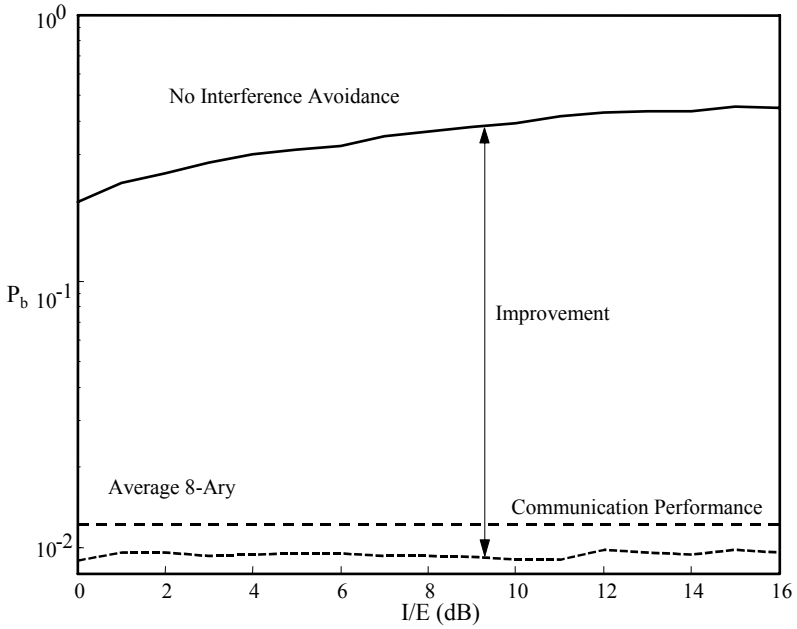

Figure 34. Average Bit Error: 8-Ary CSK Modulation Single and Multiple-tone Interference.

4.5.3 Bit Error Sensitivity Characterization for Geographically Separated Transceivers.

Previous WDCS research assumed the communicating transceivers were within a localized geographical region such that nearly identical basis functions were created for communicating. However, if the transceivers have sufficient geographical separation, they are more likely to produce dissimilar basis functions and the WDCS becomes more susceptible to bit error. For this work, the packet based WDCS robustness is addressed for two scenarios:

1. The remote transceivers produce a spectral notch of the same *width* but the *location* is inconsistent. This scenario simulates the effects of Doppler variation and multipath that may exist at both locations.

2. The remote transceivers produce a notch at the same *location* but the *width* is inconsistent. This scenario simulates the effects that may be experienced when operating over a fading channel.

Scenario 1 was simulated using 10% partial band interference. The transmitting transceiver generates a basis function for an environment containing 10% partial band interference at a relative center frequency of 0. The receiving transceiver generates a basis function for an environment containing 10% partial band interference at a relative center frequency that is offset from that of the transmitter – the relative center frequency offset ranged from –100 to 127. Two things occur under this scenario, including, 1) the transmitted communication symbols *contain energy* in spectral regions that are nulled out by the receiver (effectively a loss of desired signal energy), and 2) the transmitted communication symbols *contain no energy* in spectral regions that the receiver has not nulled-out (effectively an increase in undesired noise energy) – the net result of these two effects is a decrease in the detection SNR used for symbol estimation. Cleary, the worst case occurs when the two interference sources do not share any common spectral components, i.e., there is no spectral overlap between the two interference sources and the system experiences a net detection energy loss of approximately 10% which effectively lowers the received E_b/N_0 into the detection process.

Binary CSK results for Scenario 1 are presented in Figure 35 and clearly show optimal performance when the center frequency offset is 0, i.e., the transmitter and receiver observe identical interference and generate identical basis functions. Figure 35 also shows that the proposed packets-based WDCS is fairly robust and is capable of effectively communicating under non-ideal, 'real-world' conditions. As shown, bit error

performance degrades as the frequency offset deviates from perfect alignment. However, the indicated WDCS P_b performance is better than the case with no interference avoidance mechanisms applied for all frequency offsets considered. The following average performance results were calculated using data from the entire surface of Figure 35 in the manner illustrated by the representative cross-sectional view in Figure 36. The data indicate an average demonstrated *improvement,* relative to the no interference avoidance case, of approximately 5.4 dB, and an average *degradation* from achievable communication performance of approximately 2.3 dB. Detailed results for Scenario 1 using 4-*Ary* and 8-*Ary* CSK data modulations are provided in Appendix A and summarized in Table 3.

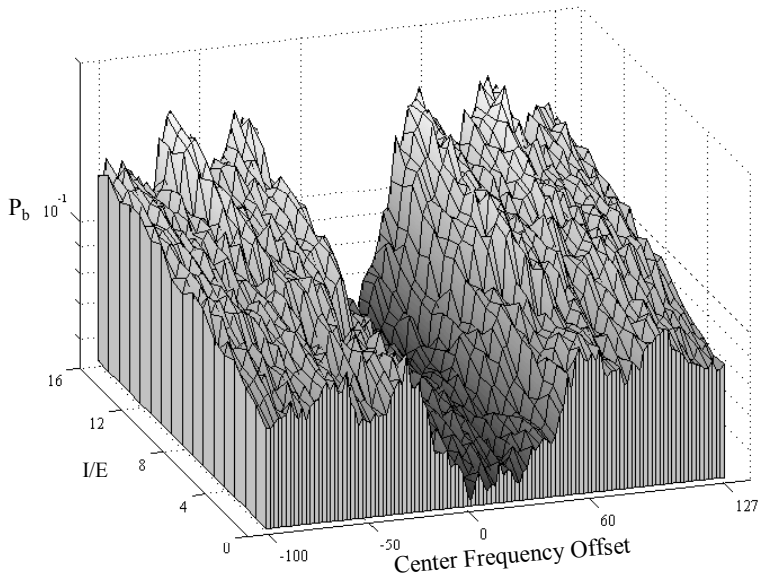

Figure 35. Scenario 1: Sensitivity to Center Frequency Offset: BCSK
E_b/N_0 = 4.0 dB

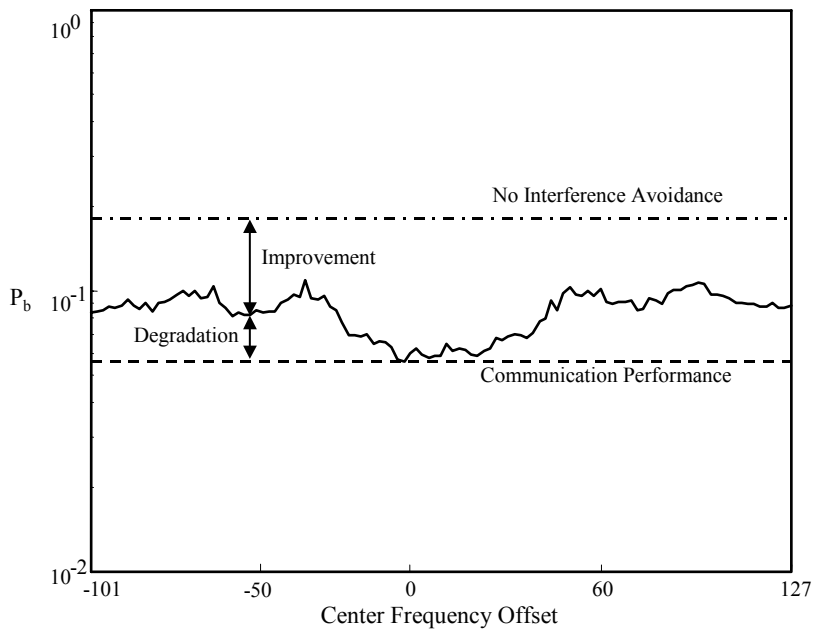

Figure 36. Scenario 1: Sensitivity to Center Frequency Offset: BCSK Cross-sectional View for I/E = 0.0 dB and E_b/N_0 = 4.0 dB

Scenario 2 was also simulated using a partial band interference source. In this case, the transmitting transceiver generates a basis function for an environment containing 10% partial band interference. Unlike Scenario 1, the center frequency of the partial band interference is identical at both transceiver locations and is held constant. In this scenario, the receiving transceiver generates a basis function for an environment containing 10% partial band interference having a spectrum with *variable width*. The interference width at the receiver is k times that of the transmitter. Except for the $k = 1$ case, the receiver nulls out spectral regions containing desired signal energy and detection E_b/N_0 effectively decreases. For this scenario, the worst case simulated was for $k = 7$, i.e., the receiver estimates the spectrum for 70% partial band interference resulting in a received energy loss of approximately 60%, significantly lowering E_b/N_0.

Binary CSK results for Scenario 2 are presented in Figure 37 and clearly show optimal performance when $k = 1$, i.e., the transmitter and the receiver generate identical basis functions. Figure 37 results indicate the proposed packet-based WDCS sustains effective communications under non-ideal, 'real-world' conditions even with a received signal energy loss of nearly 60%. The following average performance results were calculated using data from the entire surface of Figure 37 in the manner illustrated by the representative cross-sectional view of Figure 38. The data indicate an average demonstrated *improvement,* relative to the no interference avoidance case, of approximately 5.5 dB, and an average *degradation* from achievable communication performance of approximately 2.1 dB. Detailed results for Scenario 2 using 4-*Ary* and 8-*Ary* CSK data modulations are provided in Appendix A and summarized in Table 3.

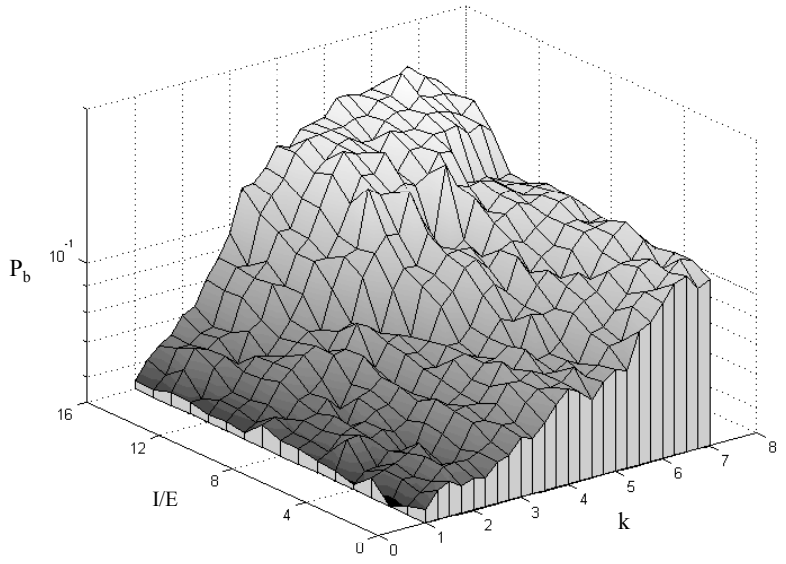

Figure 37. Scenario 2: Sensitivity to Width of Interference: BCSK
E_b/N_0 = 4.0 dB

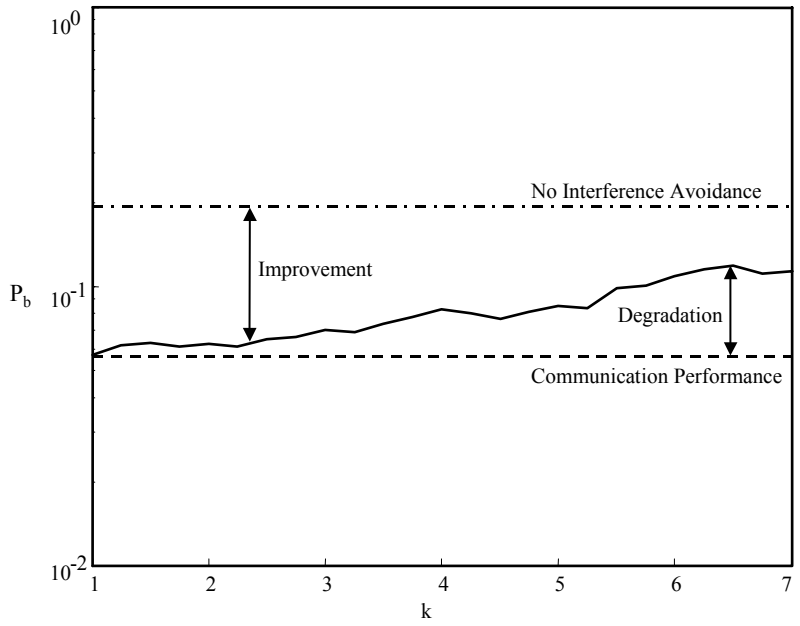

Figure 38. Scenario 2: Sensitivity to Width of Interference: BCSK Cross-sectional view for I/E = 0.0 dB and E_b/N_0 = 4.0 dB

4.6 Summary

This chapter presented simulation results and analyses for the proposed packet-based WDCS. First, the WDCS basis function was characterized and analyzed to explore the relationship between the basis function and the communication symbols. Communication symbol cross-correlation properties were then analyzed for different interference sources, the results of which partially explain the degradation seen in system performance. Wavelet representations of all simulated interference sources were then provided and a second potential source of performance degradation was identified in the wavelet packet decomposition and thresholding process. Simulation results were next provided for all simulated interference scenarios for binary, 4-*Ary*, and 8-*Ary* CSK data

modulations. A performance summary of WDCS performance is presented in Table 2. *Average Communication Performance* data (no interference present) was generated from data in Figure 21 and obtained by comparing theoretical and simulated results over the range of E_b/N_0 values condsidered. Table 2 also includes *Average Suppression Improvement* data (relative to no suppression cases) for all interference scenarios and was obtained by averaging over the range of *I/E* values considered. Table 3 summarizes the sensitivity analysis results for two simulated scenarios, including, 1) partial band, notch center frequency offset (fixed notch width) resulting from Doppler variation and multipath, and 2) partial band, notch width variations (fixed center frequency) resulting from frequency dependant fading channel effects. Finally, a performance comparison was made with original WDCS results (only binary data available) as a means of validating proposed packet-based WDCS performance. As shown in Figure 39, the proposed packet-based WDCS performs slightly better (0.1 to 0.6 dB) than the original WDCS for all scenarios considered.

Table 2. Summary of Average WDCS Performance for Various *M-Ary* CSK Modulations [12, 19]

Type of CSK Modulation	No Interference Present *Communication Performance* Variation from Bound	Interference Present and Avoidance Mechanisms Applied *Bit Error Rate Improvement*	
		Partial Band and Swept-Tone	Single and Multiple-Tone
Binary	~ 10^{-3}	6.7 dB	8.0 dB
4-*Ary*	~ 10^{-3}	9.2 dB	12.4 dB
8-*Ary*	~ 10^{-3}	12.0 dB	15.7 dB
Original BCASK	10^{-3}	6.6 dB	7.4 dB

Table 3. Summary of Average WDCS Sensitivity Analysis for various *M-Ary* CSK Modulations

Type of CSK Modulation	Interference Present and Avoidance Mechanisms Applied			
	Bit Error Rate *Improvement* over No Avoidance Case		Bit Error Rate *Degradation* from Communication Performance	
	Scenario 1	Scenario 2	Scenario 1	Scenario 2
Binary	5.4 dB	5.5 dB	2.3 dB	2.1 dB
4-*Ary*	5.2 dB	5.1 dB	6.1 dB	5.7 dB
8-*Ary*	5.9 dB	5.7 dB	8.1 dB	7.5 dB

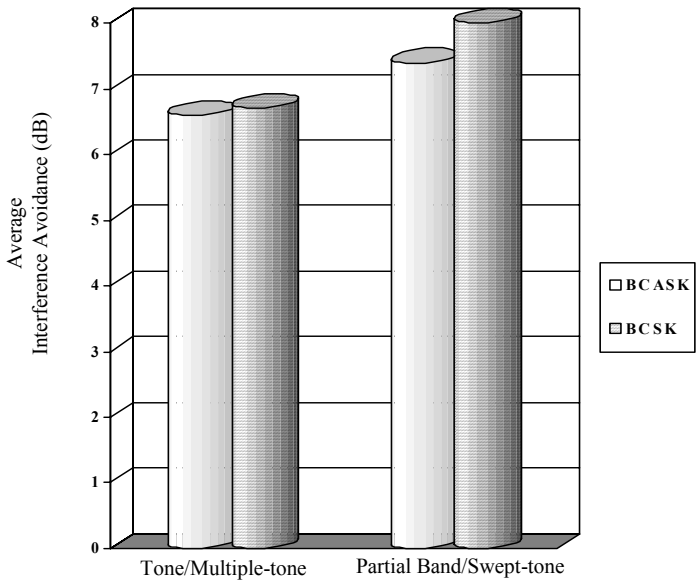

Figure 39. Average Interference Avoidance Comparison: Original WDCS (BCASK) vs. Proposed Packet-Based WDCS (BCSK).

5 Conclusions and Recommendations

5.1 Summary

Simulation results indicate the proposed packet-based WDCS provides acceptable *M-Ary* orthogonal cyclic shift keyed (CSK) communication performance while offering considerable interference avoidance capability. Bit error (P_b) performance analysis for several interference scenarios, including single-tone, multiple-tone, swept-tone, and partial band interference, revealed the WDCS architecture using a wavelet packet decomposition technique is highly capable of 'avoiding' interference, i.e., estimating and mitigating interference effects. WDCS performance was simulated using MATLAB® at an average signal bit energy-to-noise power spectral density (PSD) level (E_b/N_0) of 4.0 dB and average interference-to-average signal energy (I/E) levels ranging from 0.0 dB to 16.0 dB. For binary, 4-*Ary*, and 8-*Ary* CSK data modulations, the packet-based WDCS exhibited average P_b improvements (indicative of interference avoidance capability) of 6.7, 9.2, and 12.0 dB, respectively, for partial band and swept-tone interference. For single and multiple-tone interference, P_b improvements of 8.0, 12.4, and 15.7 dB were realized for binary, 4-*Ary*, and 8-*Ary* CSK data modulations, respectively. Furthermore, bit error sensitivity analysis indicates the WDCS is capable of communicating effectively under non-ideal 'real-world' conditions (geographically separated transceivers immersed in dissimilar electromagnetic environments) while exhibiting average P_b improvements of 5.4, 5.1, and 5.8 dB relative to systems having no interference avoidance capability.

5.2 Recommendations for Future Research

The packet-based WDCS simulation results indicate the system is a robust, practical interference avoidance communication system that warrants further consideration for operational applications. To this end, further research in the following areas will enhance system effectiveness and aid the transition to operational status. Potential future research topic areas include:

1. A detailed investigation into the design of an adaptive thresholding process.
2. Additional sensitivity analysis for geographically separated transceivers immersed in dissimilar electromagnetic environments.
3. Hardware-in-the-loop characterization and demonstration of WDCS performance using the GP-3 transceiver analysis system or other available communication equipment.

To date, WDCS research has used a fixed thresholding scheme whereby the threshold level is set at 20% above the received noise power level – although effective for demonstration purposes, no claims of optimality have been made with regard to this particular scheme. As identified in Chapter 4, a fixed thresholding scheme introduces some inefficiencies in the thresholding/spectral estimation process and can produce sub-optimal performance. Implementation of an adaptive thresholding scheme could produce more effective interference estimates in environments containing both low and high power spectral components. A threshold level could be adaptively generated based on

the power contained in a predetermined number of wavelet coefficients or on power in individual sub-bands.

The sensitivity analysis of this work was limited and only considered partial band interference for two scenarios, including simulation of 1) the effects of Doppler variation and multipath, and 2) the effects that may be experienced while operating over a fading channel. These two scenarios could easily be expanded to include additional interference sources such as the sinusoidal tone interferers. The goal of further sensitivity analyses should remain focused on the geographically separated transceivers immersed in dissimilar electromagnetic environments – the key is to demonstrate reliable communication performance while inducing basis function dissimilarity at the transceiver locations. Additional scenarios not examined in this work could include modeling scenarios containing a large number of interference sources.

1. Include additional interferers at the *receiver* location that are not contained in the local geographical region of the transmitter, or equivalently, the additional interferers have insufficient power to be observed at the transmitter location.
2. Include additional interferers at the *transmitter* location that are not contained in the local geographical region of the receiver, or equivalently, the additional interferers have insufficient power to be observed at the receiver location.

Finally, demonstration of WDCS communication performance with developmental hardware would lend credibility to the system and be a giant step towards obtaining a realizable system. Partial system implementation would be cost effective and provide valuable insight into 'real-world' synchronization, demodulation, and communication performance issues.

Appendix A – Additional Sensitivity Analysis Data

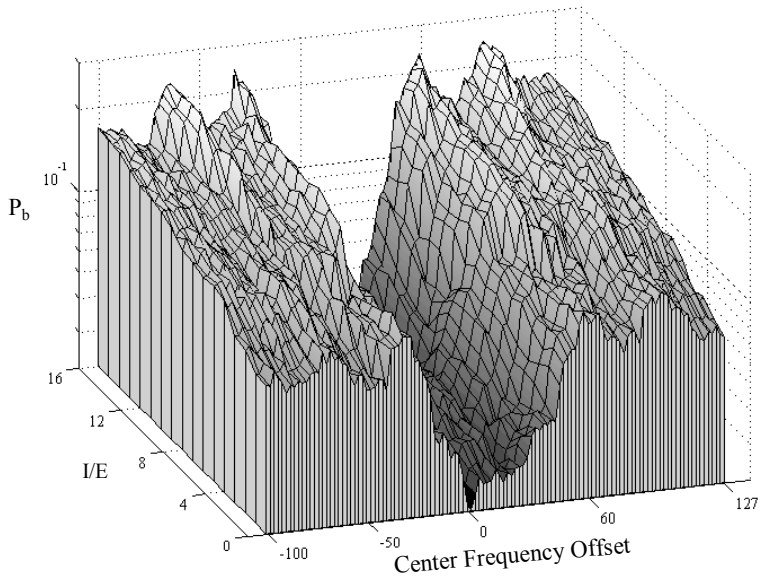

Figure 40. Scenario 1: Sensitivity to Center Frequency Offset: 4-Ary CSK E_b/N_0 = 4.0 dB

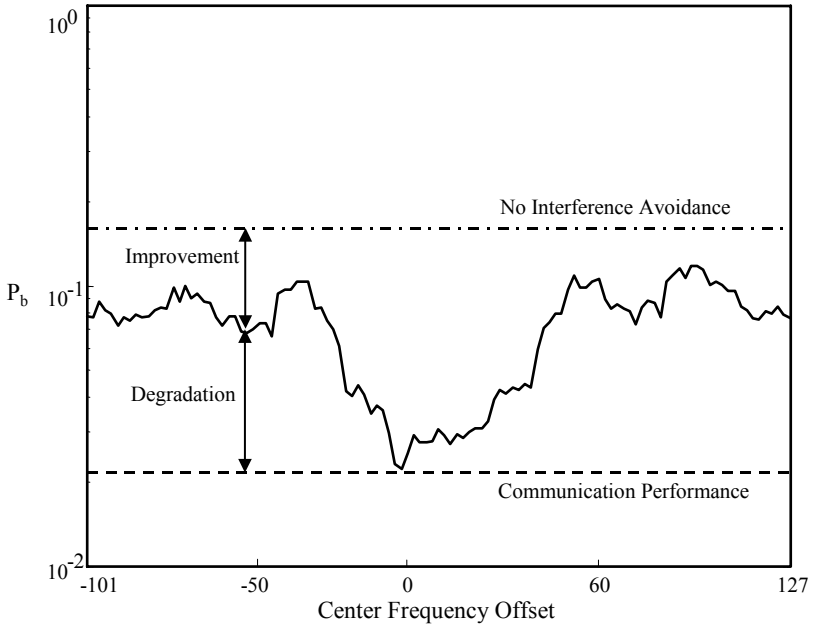

Figure 41. Scenario 1: Sensitivity to Center Frequency Offset: 4-Ary CSK Cross-Sectional View for I/E = 0.0 dB and E_b/N_0 = 4.0 dB

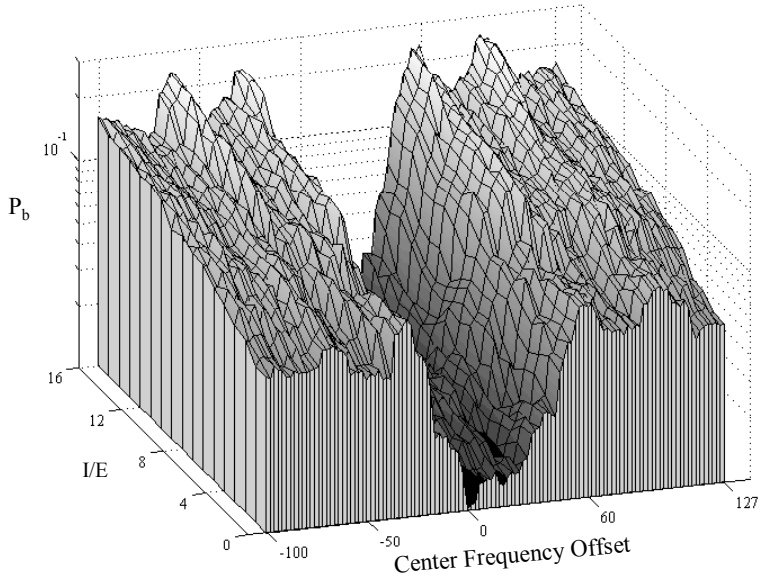

Figure 42. Scenario 1: Sensitivity to Center Frequency Offset: 8-Ary CSK E_b/N_0 = 4.0 dB.

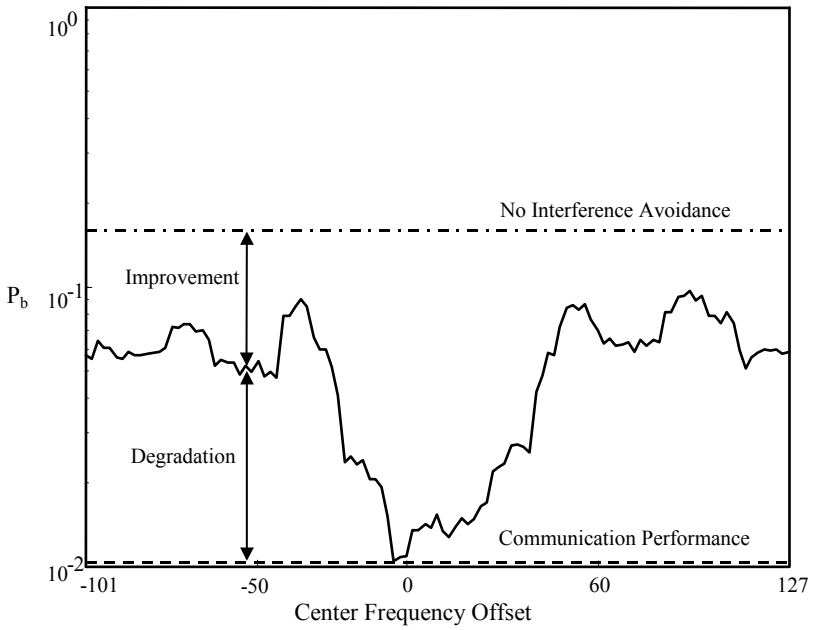

Figure 43. Scenario 1: Sensitivity to Center Frequency Offset: 8-Ary CSK Cross-Sectional View for I/E = 0.0 dB and E_b/N_0 = 4.0 dB.

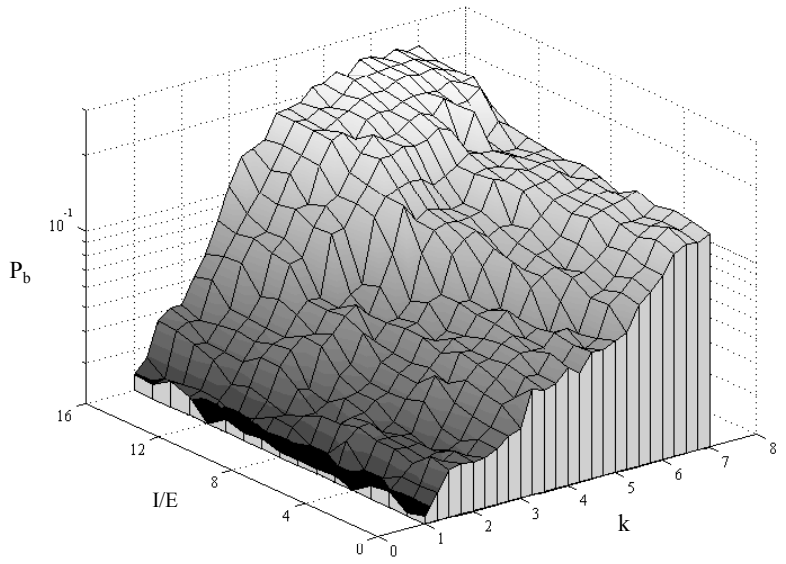

Figure 44. Scenario 2: Sensitivity to Width of Interference: 4-Ary CSK E_b/N_0 = 4.0 dB

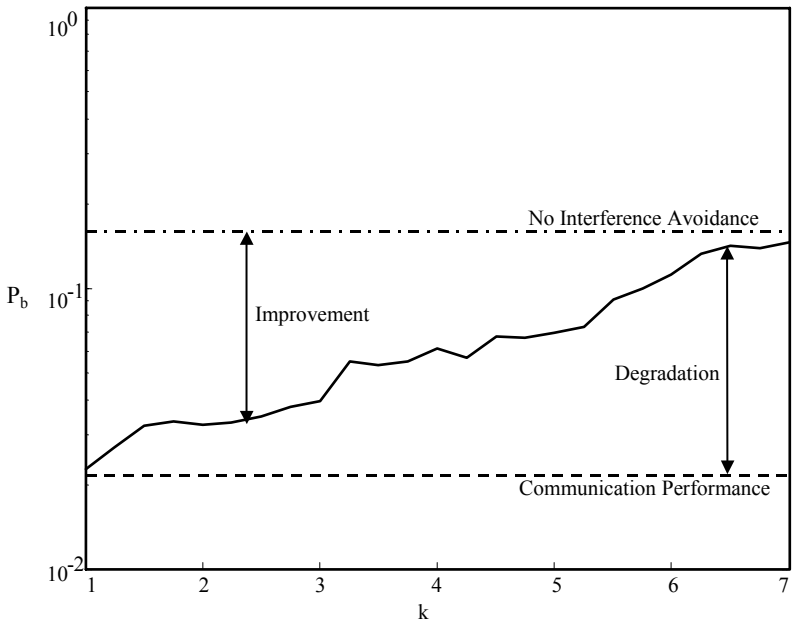

Figure 45. Scenario 2: Sensitivity to Width of Interference: 4-Ary CSK Cross-Sectional View for I/E = 0.0 dB and E_b/N_0 = 4.0 dB

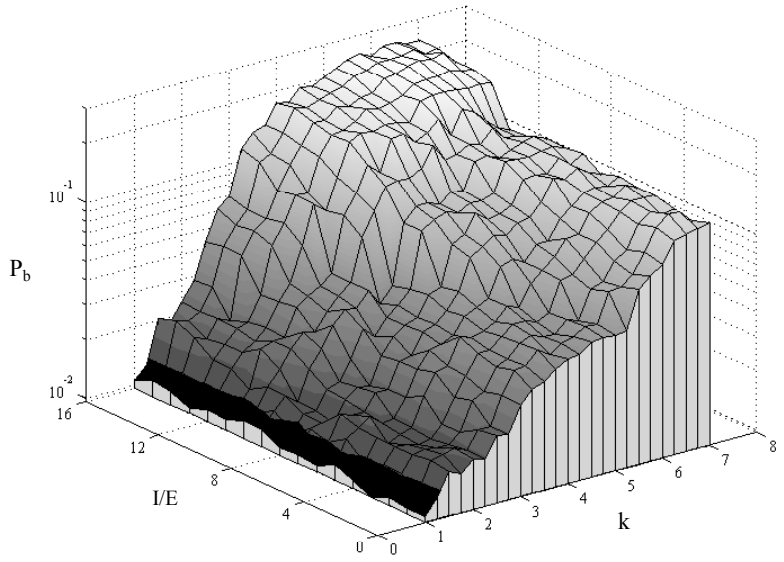

Figure 46. Scenario 2: Sensitivity to Width of Interference: 8-Ary CSK E_b/N_0 = 4.0 dB

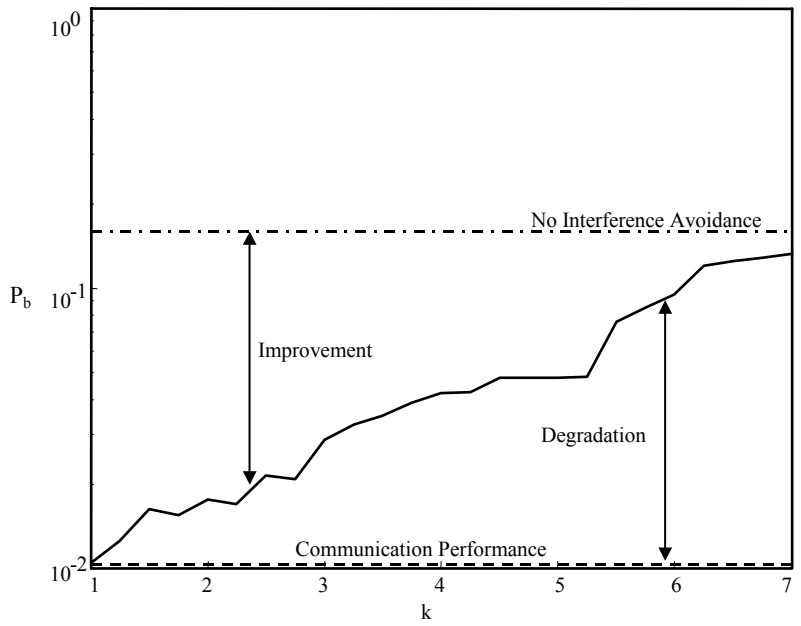

Figure 47. Scenario 2: Sensitivity to Width of Interference: 8-Ary CSK Cross-Sectional View for I/E = 0.0 dB and E_b/N_0 = 4.0 dB

Appendix B – MATLAB® Code

All of the MATLAB® files used for this research are listed below with brief descriptions. The code developed for the wavelet packet implementation is given in full.

- *create_noise.m* -- Creates a noisy channel environment by adding AWGN with an interference signal.
- *daub.m* -- Computes the Daubechies scaling coefficients.
- *db.m* -- Converts an absolute number to a decibel value.
- *dec2bin.m* -- Returns the binary representation of the decimal input number.
- *dwpt.m*

```
function g = dwpt(f,h,NJ)
% function g = dwpt(f,h,NJ)  Calculates the DWPT of periodic f
% with scaling filter h and NJ scales.

N = length(h);
L = length(f);
data = f;
g = [];

%Determines number of scales if none provided in input
if isempty(NJ)
  NJ = round(log10(L)/log10(2));
end

%Scaling Filter -- Lowpass
h0 = fliplr(h);  %sum of h[n] = sqrt(2)

%Wavelet Filter -- Highpass
h1 = h;
h1(1:2:N) = -h1(1:2:N);

for j = 1:NJ
     for k = 1:2^(j-1)

      width = L/(2^j);
      data1 = data([1: (2*width)] + (k-1)*2*width);

      %Make periodic
      data2 = [data1(mod((-(N-1):-1),2*width)+1) data1];

      %Convolve and down sample
      d = conv(data2,h1);
      d = d(N:2:(N+2*width-2));
```

```
      c = conv(data2,h0);
      c = c(N:2:(N+2*width-2));

      data((1 + (k-1)*2*width) : (width+ (k-1)*2*width)) = c;
      data([(1 + (k-1)*2*width) : (width + (k-1)*2*width)]+width) = d;

    end
  end

%The DWPT
g = [data];
```

- *dwpt_thresh.m*

```
function g = dwpt_thresh(f,h,NJ,L,N)
% function g = dwpt_thresh(f,h,NJ,L,N)  Calculates the DWPT of periodic % f  with scaling filter h and NJ scales.  The DWPT coefficients are then
% passed through a thresholding process to generate a notched waveform % A'(w) of ones and zeros.
% f - input signal
% h - filter coefficients
% NJ - number of scales
% L - number of symbols
% N - number of samples per symbol

Nh = length(h);
Lf = length(f);
data = f;
g = [];
x = zeros(1,2*NJ);
data_thresh = zeros(1,N);

%Determines number of scales if none provided in input
if isempty(NJ)
  NJ = round(log10(Lf)/log10(2));
end

%Scaling Filter -- Lowpass
h0 = fliplr(h);  %sum of h[n] = sqrt(2)

%Wavelet Filter -- Highpass
h1 = h;
h1(1:2:Nh) = -h1(1:2:Nh);

for j = 1:NJ
    for k = 1:2^(j-1)

      width = Lf/(2^j);
      data1 = data([1: (2*width)] + (k-1)*2*width);

      %Make periodic
      data2 = [data1(mod((-(N-1):-1),2*width)+1) data1];

      %Convolve and down sample
```

```
        d = conv(data2,h1);
        d = d(Nh:2:(Nh+2*width-2));
        c = conv(data2,h0);
        c = c(Nh:2:(Nh+2*width-2));

        data((1 + (k-1)*2*width) : (width+ (k-1)*2*width)) = c;
        data([(1 + (k-1)*2*width) : (width + (k-1)*2*width)]+width) = d;

        % Determine power in the subband and apply the threshold.
        % If the signal power exceeds the noise power by 20 percent,
        % interference is declared present and the subband is nulled
        % out (coefficients set to zero).  If there is no interference
        % the subband is retained (coefficients set to one).

        L2_c = sum((abs(c).^2))/width;  %L2 metric
        L2_d = sum((abs(d).^2))/width;  %L2 metric

        if L2_c < 1.2
            data_thresh((1 + (k-1)*2*width/L) : (width/L+ (k-1)*2*width/L)) = 1;
        end

        if L2_d < 1.2
           data_thresh([(1 + (k-1)*2*width/L) : (width/L + (k)*2*width/L)]+width/L) = 1;
        end
      end
end

g = data_thresh;  % A'(w)
```

- *eb_no_correlation.m* -- Incorporates cross-correlation effects for binary orthogonal signaling.
- *eb_no_plot.m* -- Plots theoretical and simulated P_b values to validate communication performance of the model. Also outputs the mean absolute error and standard deviation between the theoretical and simulated P_b values.
- *idwpt.m*

```
function f = idwpt(g,h,NJ)
% function f = idwpt(g,h,NJ)  Calculates the IDWPT of periodic f
% with scaling filter h and NJ scales

N = length(h);
L = length(g);

%Determines number of scales if none provided in input
if isempty(NJ)
  NJ = round(log10(L)/log10(2));
end
```

```
%Scaling Filter  -- Lowpass
h0 = h;  %sum of h[n] = sqrt(2)

%Wavelet Filter  -- Highpass
h1 = fliplr(h);
h1(2:2:N) = -h1(2:2:N);
data=g;

for j = NJ:-1:1
   for k = 2^(j-1):-1:1

     width=L/(2^j);

      %Make periodic
      w = mod(0:N/2-1,width)+1;

      %Wavelet Coeffs
      data1=data([1: 2*width] + (k-1)*2*width);
      data2=data1(1+width:2*width);
      data1=data1(1:width);

      %Up sample & periodic
      cu(1:2:2*width+N) = [data1 data1(1,w)];
      du(1:2:2*width+N) = [data2 data2(1,w)];

      %Convolve and combine
      c = conv(cu,h0) + conv(du,h1);
      c = c(N:N+2*width-1);
      data([1:2*width] + (k-1)*2*width) = c;

  end
end

%The IDWPT
f = data;
```

- *invdb.m* -- Converts a decibel value to an absolute number.
- *masterp.m* -- Master simulation code to simulate the packet-based WDCS for M-*Ary* CSK.
- *master.m* -- Master simulation code to simulate the original WDCS for Antipodal, BCSK, and BCASK.
- *matshift.m* -- Progressive shift of a matrix.
- *notchcenterfreq.m* -- This code simulates 10 % partial band interference seen by the transmitter at f_j and offsets the center frequency of the partial band jammer seen by the receiver. Simulates Scenario 1.

- *notchwidth.m* -- This code simulates a 10 % partial band jammer seen by the transmitter *and* receiver at f_j and changes the width of the partial band jammer seen by the receiver. Simulates Scenario 2.
- *oct2bin.m* -- Returns the binary representation of the octal input number.
- *pershift.m* -- Periodic end-around shift a row vector.
- *pn.m* -- Generates a pseudorandom sequence.
- *pr_phase.m* -- Returns a complex vector of pseudo random phases.
- *q.m* -- The Complementary Error Function, a.k.a, the *Q* Function.
- *r_dwt.m* -- Calculates the DWT of periodic f with scaling filter h and NJ scales.
- *r_dwt_thresh.m* -- Calculates the DWT of periodic f with scaling filter h and NJ scales. The DWT coefficients are then passed through a thresholding process to generate a notched waveform $A'(\omega)$ of ones and zeros.
- *r_idwt.m* -- Calculates the IDWT of periodic f with scaling filter h and NJ scales.
- *rho.m* -- Calculates the cross-correlation coefficients for M-*Ary* CSK.
- *run_average_rho.m* -- Calculates the average cross-correlation coefficients for M-*Ary* CSK using rho.m.
- *runall_center_width.m* -- Runs all of the Scenario 1 and 2 simulations.
- *runallw.m* -- Runs all of the interference scenarios for the original WDCS.
- *runallwp.m* -- Runs all communication validation simulations and all interference scenarios for the packet-based WDCS.

Bibliography

1. Radcliffe, Rodney A. Design and Simulation of a Transform Domain Communication System. MS Thesis, AFIT/GE/ENG/96D-16, Air Force Institute of Technology, Wright-Patterson AFB OH, December 1996.

2. Klein, Randall W. Wavelet Domain Communication System (WDCS): Design, Model, Simulation, and Analysis. MS Thesis, AFIT/GE/ENG/01M-16, Air Force Institute of Technology, Wright-Patterson AFB OH, March 2001.

3. Milstein, Arsenault, Das. "Transform Domain Processing for Digital Communications Systems Using Surface Acoustic Wave Devices." Technical Report, Troy, NY: Contract: Army DAAG-29-77-G-0205, May 1978.

4. Milstein, Arsenault, Das. "Processing Gain Advantage of Transform Domain Filtering DS – Spread Spectrum Systems." MILCOM '82, October 1982.

5. German, Edgar H. "Transform Domain Signal Processing Study Final Report." Technical Report, Reistertown MD: Contract: Air Force F30602-86-C-0133, August 1988.

6. Andren, Carl F., et al. Low Probability-of-Intercept Communication System. Harris Corporation, U.S. Patent 5 029 184, 1991.

7. Swackhammer, Patrick J. Design and Simulation of a Multiple Access Transform Domain Communication System. MS Thesis, AFIT/GE/ENG/99M-28, Air Force Institute of Technology, Wright-Patterson AFB OH, March 1999.

8. Radcliffe, Rodney A. and Gerald C Gerace. "Design and Simulation of a Transform Domain Communication System." MILCOM '97, October 1997.

9. Roberts, Marcus L. Synchronization of a Transform Domain Communication System. MS Thesis, AFIT/GE/ENG/00M-15, Air Force Institute of Technology, Wright-Patterson AFB OH, March 2000.

10. Peterson, Roger L., et al. Introduction to Spread Spectrum Communications. New Jersey: Prentice Hall, 1995.

11. Sklar, Bernard. Digital Communications: Fundamentals and Applications. New Jersey: Prentice Hall, 1988.

12. Klein, Randall W., et al., "Performance Characterization of a Proposed Wavelet Domain Communications System (WDCS)," 5th World Multi-Conference on Systemics, Cybernetics and Informatics, SCI '01, July 2001.

13. Burrus, C. Sidney, et al. Introduction to Wavelets and Wavelet Transforms: A Primer. New Jersey: Prentice Hall, 1998.

14. Daubechies, "Ten Lectures on Wavelets," *SIAM*, Philadelphia, PA, 1992.

15. Ziemer, R.E. and W.H. Tranter. Principles of Communication: Systems, Modulation, and Noise: Third Edition. Boston: Houghton Mifflin Company, 1990.

16. Jeruchim, M.C., P. Balaban, and K. S. Shanmugan. Simulation of Communication Systems. New York: Plenum Press, 1992.

17. Coifman, R.R. and M.V. Wickerhauser. "Entropy Based Algorithms for Best Basis Selection," *IEEE Transactions on Information Theory*, vol. 32, num. 2, pp. 712-718, March 1992.

18. Proakis, J.G., Digital Communications. 4th Edition, New York: McGraw-Hill, 2001.

19. Lee, Marion Jay F., et al., "Transform Domain Communications and Interference Avoidance Using Wavelet Packet Decomposition," IEEE Wireless Communications and Networking Conference, WCNC '02, March 2002.

REPORT DOCUMENTATION PAGE

Form Approved
OMB No. 074-0188

1. REPORT DATE *(DD-MM-YYYY)*	2. REPORT TYPE	3. DATES COVERED *(From – To)*
07-03-2002	**Master's Thesis**	Jun 2001 – Mar 2002

4. TITLE AND SUBTITLE

WAVELET DOMAIN COMMUNICATION SYSTEM (WDCS): PACKET-BASED WAVELET SPECTRAL ESTIMATION AND M-ARY SIGNALING

5a. CONTRACT NUMBER

5b. GRANT NUMBER

5c. PROGRAM ELEMENT NUMBER

6. AUTHOR(S)

Marion Jay F. Lee, First Lieutenant, USAF

5d. PROJECT NUMBER

5e. TASK NUMBER

5f. WORK UNIT NUMBER

7. PERFORMING ORGANIZATION NAMES(S) AND ADDRESS(S)
Air Force Institute of Technology
Graduate School of Engineering and Management (AFIT/EN)
2950 P Street, Building 640
WPAFB OH 45433-7765

8. PERFORMING ORGANIZATION REPORT NUMBER

AFIT/GE/EMG/02M-14

9. SPONSORING/MONITORING AGENCY NAME(S) AND ADDRESS(ES)
AFRL/SNRW
Attn: Mr. James P. Stephens
2241 Avionics Cl, Bldg. 620 Rm. N2-L3 DSN: 785-5579 x 4239
WPAFB OH 45433-7765 e-mail: james.stephens@wpafb.af.mil

10. SPONSOR/MONITOR'S ACRONYM(S)

11. SPONSOR/MONITOR'S REPORT NUMBER(S)

12. DISTRIBUTION/AVAILABILITY STATEMENT

APPROVED FOR PUBLIC RELEASE; DISTRIBUTION UNLIMITED.

13. SUPPLEMENTARY NOTES
AFIT Technical POC: Michael A. Temple, AFIT/ENG
michael.temple@afit.edu

14. ABSTRACT

A recently proposed Wavelet Domain Communication System (WDCS) using transform domain processing demonstrated excellent interference avoidance capability under adverse environmental conditions. This work extends previous results by 1) incorporating a wavelet packet decomposition technique, 2) demonstrating *M-Ary* signaling capability, and 3) providing increased adaptivity over a larger class of interference signals. The newly proposed packet-based WDCS is modeled and its performance characterized using MATLAB®. In addition, the WDCS response to two scenarios simulating Doppler effects and physical separation of transceivers are obtained. The fundamental metric for analysis and performance evaluation is bit error rate (P_b). Relative to the previous non-packet WDCS, the proposed packet-based WDCS provides improved/comparable bit error performance in several interference scenarios – single-tone, multiple-tone, swept-tone, and partial band interference is considered. Interference 'avoidance' capability was characterized for a bit energy-to-noise power level (E_b/N_0) of 4.0 dB and interference energy-to-signal energy (I/E) ratios ranging from 0.0 dB to 16.0 dB. For binary, 4-*Ary*, and 8-*Ary* CSK data modulations, the packet-based WDCS exhibited average P_b improvements of 6.7, 9.2, and 12.0 dB, respectively, for partial band and swept-tone interference. For single and multiple-tone interference, improvements of 8.0, 12.4, and 15.7 dB were realized. Furthermore, bit error sensitivity analyses indicate the WDCS communicates effectively under non-ideal 'real-world' conditions (transceivers located in dissimilar environments) while exhibiting average P_b improvements of 5.4, 5.1, and 5.8 dB, relative to systems having no interference suppression.

15. SUBJECT TERMS
Interference Avoidance, Transform Domain, Wavelet Domain, Wavelets, Wavelet Packets, Communication, Cyclic Shift Keying

16. SECURITY CLASSIFICATION OF:			17. LIMITATION OF ABSTRACT	18. NUMBER OF PAGES	19a. NAME OF RESPONSIBLE PERSON
a. REPORT	b. ABSTRACT	c. THIS PAGE			Michael A. Temple, Ph.D. (ENG)
U	U	U	UU	95	19b. TELEPHONE NUMBER *(Include area code)* (937) 255-3636, ext 4703; e-mail: michael.temple@afit.edu